Biochemical and Biophysical Research Communications 374 (2008) 394–398

Contents lists available at ScienceDirect

Biochemical and Biophysical Research Communications

journal homepage: www.elsevier.com/locate/ybbrc

Podocalyxin expression in malignant astrocytic tumors

Norihito Hayatsu [a], Mika Kato Kaneko [b], Kazuhiko Mishima [c], Ryo Nishikawa [c], Masao Matsutani [c], Janet E. Price [b], Yukinari Kato [b,*]

[a] Graduate School of Medicine, Kyoto University, Yoshida-konoe-cho, Sakyo-ku, Kyoto 606-8501, Japan
[b] Department of Cancer Biology, Unit 173, University of Texas M.D. Anderson Cancer Center, 1515 Holcombe, Houston, TX 77030, USA
[c] Saitama Medical University International Medical Center, 1397-1 Yamane Hidaka-shi, Saitama 350-1298, Japan

ARTICLE INFO

Article history:
Received 4 July 2008
Available online 17 July 2008

Keywords:
Podocalyxin
Keratan sulfate
Proteoglycan
Astrocytic tumor
Glioblastoma

ABSTRACT

Podocalyxin is an anti-adhesive mucin-like transmembrane sialoglycoprotein that has been implicated in the development of aggressive forms of cancer. Podocalyxin is also known as keratan sulfate (KS) proteoglycan. Recently, we revealed that highly sulfated KS or another mucin-like transmembrane sialoglycoprotein podoplanin/aggrus is upregulated in malignant astrocytic tumors. The aim of this study is to examine the relationship between podocalyxin expression and malignant progression of astrocytic tumors. In this study, 51 astrocytic tumors were investigated for podocalyxin expression using immunohistochemistry, Western blot analysis, and quantitative real-time PCR. Immunohistochemistry detected podocalyxin on the surface of tumor cells in six of 14 anaplastic astrocytomas (42.9%) and in 17 of 31 glioblastomas (54.8%), especially around proliferating endothelial cells. In diffuse astrocytoma, podocalyxin expression was observed only in vascular endothelial cells. Podocalyxin might be associated with the malignant progression of astrocytic tumors, and be a useful prognostic marker for astrocytic tumors.

Astrocytic tumors are the most common tumors of the central nervous system (CNS) and are categorized into diffuse astrocytomas (World Health Organization (WHO) Grade II), anaplastic astrocytomas (WHO Grade III), and glioblastomas (WHO Grade IV) [1]. Glioblastoma may occur de novo or may result from progression of low-grade astrocytomas [2]. Molecular mechanisms of malignant progression are associated with inactivation of tumor suppressor genes such as p53-Rb pathway or overexpression of oncogenes such as epidermal growth factor receptor (EGFR) [3]. However, the mechanisms of malignant progression of astrocytic tumors have not been resolved completely. Identification of genes that are expressed differentially in high-grade or low-grade astrocytomas is important to elucidate the molecular mechanisms of malignant progression and to develop novel therapeutic strategies.

Podocalyxin is a type I transmembrane sialoglycoprotein, which belongs to the CD34 family. Podocalyxin is expressed on the surface of various normal cells, including kidney podocytes, vascular endothelial cells, hematopoietic stem cells, and platelets [4–7]. The physiological function of podocalyxin is as an anti-adhesion molecule that maintains open filtration pathways between neighboring podocyte foot processes through the charge-repulsive effects of its large, highly sialylated and sulfated extracellular domain [8]. In canine kidney (MDCK) cells, podocalyxin overexpression leads to the inhibition of cell–cell interaction as shown by decreased cell–cell adhesion, decreased tight junction-dependent transepithelial resistance, and redistribution of cell junction proteins [9]. Decreased cell–cell interaction is a prominent feature of cancer cells that display a metastatic phenotype, suggesting a possible role for anti-adhesive molecules, such as podocalyxin, in cancer progression. The role of podocalyxin in cancer remains unclear, although its expression has been reported in breast, liver, pancreas, kidney, prostate, testis, and blood cell cancers [10–16]. However, podocalyxin has been implicated in the development of aggressive forms of cancer. Increased podocalyxin protein expression is correlated with poor outcome in breast carcinomas, and is implicated in more aggressive forms of prostate cancer [10,14]. Furthermore, podocalyxin variants were found to be associated with both the risk of prostate cancer and prostate tumor aggressiveness. Recently, podocalyxin was reported to increase the aggressive phenotype of breast and prostate cancer in vitro through its interaction with ezrin [17]. Thus, podocalyxin is a candidate for playing a critical role in cancer aggressiveness and malignancy. Podocalyxin is also reported to be useful to differentiate pancreatic ductal adenocarcinomas from adenocarcinomas of the biliary and gastrointestinal tracts [12].

Recently, we showed that the expression of highly sulfated keratan sulfate (KS) recognized by 5D4 antibody is increased in

Abbreviations: KS, keratan sulfate; CNS, central nervous system; WHO, World Health Organization.

* Corresponding author. Fax: +81 29 861 3191.
E-mail address: yukinari-k@bea.hi-ho.ne.jp (Y. Kato).

0006-291X/$ - see front matter © 2008 Elsevier Inc. All rights reserved.
doi:10.1016/j.bbrc.2008.07.049

parallel with increasing malignancy of astrocytic tumors [18,19]. KS expression is induced by high expression of five glycogenes involved in KS synthesis. However, in addition to high expression levels of glycogenes involved in KS synthesis, core proteins of KS proteoglycan also might contribute to the high expression of KS. Podocalyxin was recently identified as a KS proteoglycan [20]. In this study, 51 astrocytic tumors (six diffuse astrocytomas, 14 anaplastic astrocytomas, and 31 glioblastomas) were investigated using immunohistochemistry and Western blot with an anti-podocalyxin antibody. Furthermore, we investigated the podocalyxin transcript levels using quantitative real-time PCR in 51 frozen astrocytic tumors.

Materials and methods

Tissue samples. Tumor specimens were obtained during surgery from six patients with diffuse astrocytomas, 14 patients with anaplastic astrocytomas, and 31 patients with glioblastomas [19,21]. Informed consent had been obtained previously from patients or their guardians. The histology of these tissue samples was confirmed by experienced neuropathologists.

Immunohistochemical analysis. Specimens were deparaffinized, rehydrated and incubated first with goat anti-human podocalyxin (2 μg/ml) at 4 °C for 18 h, then with biotin-conjugated secondary anti-goat IgG antibody (Dako, Glostrup, Denmark) for 1 h, and finally with peroxidase-conjugated biotin-streptavidin complex (Vectastain ABC Kit; Vector Laboratories Inc., Burlingame, CA) for 1 h. Color was developed using 3, 3-diaminobenzidine tetrahydrochloride tablet sets (Dako) for 3 min. KS expression was assessed semi-quantitatively from the percentage of tumor cells with cytoplasmic/membrane staining: 0, no staining; +, <10%; ++, 10–50%; and +++, >50%.

Western blot analysis. The tissues were lysed with lysis buffer (25 mM Tris (pH 7.4), 50 mM NaCl, 0.5% Na deoxycholate, 2% Nonidet P-40, 0.2% SDS, 1 mM phenylmethylsulfonyl fluoride, and 50 mg/ml aprotinin) [19,21]. Samples of the supernatant fraction were collected after centrifuging at 15,000g for 30 min. Four micrograms of the proteins were electrophoresed under reducing conditions on 10% polyacrylamide gel (Atto Bioscience, Tokyo, Japan). The separated proteins were transferred to a PVDF membrane. After blocking with 3% skim milk in PBS with 0.05% Tween 20, the membrane was incubated with goat anti-human podocalyxin (0.1 μg/ml; R&D Systems, Minneapolis, MN) or anti-β-actin antibody (1/5000 dilution; Sigma, St. Louis, MO), and subsequently with peroxidase-conjugated anti-goat or anti-mouse antibodies (1/5000 dilution; Bio-Rad Laboratories Inc., Hercules, CA). It was then developed for 1 min with ECL reagents (Amersham Pharmacia Biotech Inc.) using Amersham Hyperfilm ECL (Amersham Pharmacia Biotech Inc.).

Quantitative real-time PCR analysis. Total RNAs were prepared from 51 astrocytic tumors (six diffuse astrocytomas, 14 anaplastic astrocytomas, and 31 glioblastomas) using an RNeasy mini prep kit (Qiagen Inc., Hilden, Germany). The initial cDNA strand was synthesized using SuperScript III transcriptase (Invitrogen Corp., Carlsbad, CA) by priming an oligo-dT primer according to the manufacturer's instructions. We performed PCR using oligonucleotides: human podocalyxin sense (5′-acaggaaacaccctctgtgc-3′) and human podocalyxin antisense (5′-gaaggtggctttgactgctc-3′). Real-time PCR was carried out using the QuantiTect SYBR Green PCR (Qiagen Inc.). The PCR conditions were 95 °C for 15 min (1 cycle), followed by 40 cycles of 94 °C for 15 s, 53 °C for 20 s, and 72 °C for 10 s. Subsequently, a melting curve program was applied with continuous fluorescence measurement. A standard curve for podocalyxin templates was generated through serial dilution of PCR products (1×10^8 to 1×10^2 copies/μl). The expression level of podocalyxin was normalized by total RNA weights. The statistical significance of podocalyxin mRNA expression in astrocytic tumor tissues was determined using paired *t* tests.

Statistical analyses. Results are expressed as the mean ± standard deviation. Student's *t*-test was used to determine significance among the groups. A value of $p < 0.05$ was considered significant.

Results

Immunohistochemical staining for podocalyxin in malignant astrocytic tumors

The cellular distribution of podocalyxin in astrocytic tumors was examined immunohistochemically using goat anti-human podocalyxin polyclonal antibody. This polyclonal antibody was produced in goats immunized with recombinant human podocalyxin extracellular domain (23–425 a.a.), and purified using podocalyxin affinity chromatography. In many recent studies, this antibody was applied to the immunohistochemistry, Western blot, and immunoprecipitation, indicating that this antibody is specific to human podocalyxin [20,22,23]. Herein, we used 51 surgical tissue samples (six diffuse astrocytomas: Grade II, 14 anaplastic astrocytomas: Grade III, and 31 glioblastomas: Grade IV) for immunohistochemistry. Podocalyxin immunoreactivity was detected in six of 14 (42.9%) anaplastic astrocytomas and in 17 of 31 (54.8%) glioblastomas; staining was graded as +++ in seven glioblastoma and as ++ in three glioblastoma cases (Table 1). Podocalyxin was not detected on tumor cell surfaces in diffuse astrocytomas, yet was observed in vascular endothelial cells in these specimen (Fig. 1A and B). Representative staining for podocalyxin in astrocytic tumor samples is shown in Fig. 1. Immunostaining for podocalyxin demonstrated predominantly cell-surface patterns. In anaplastic astrocytoma, the tumor cell surface was stained using anti-podocalyxin (Fig. 1C and D). In glioblastomas, podocalyxin-positive tumor cells were prominent around microvascular proliferations (Fig. 1E and F). Proliferating endothelial cells were also positive for podocalyxin (Fig. 1F).

Analysis of podocalyxin expression using Western blot in astrocytic tumors

To confirm the podocalyxin expression in astrocytic tumors, lysates of frozen tumor specimens from 51 patients were analyzed using Western blot analysis with anti-podocalyxin antibody. As shown in Fig. 2, podocalyxin was highly detected in extracts of anaplastic astrocytoma and glioblastoma. Samples of one of 14 anaplastic astrocytomas (7.1%) and seven of 31 glioblastomas (22.6%) showed relatively high levels of podocalyxin, while expression in five of 14 anaplastic astrocytomas (35.7%) and 11 of 31 glioblastomas (35.5%) was more moderate. The other astrocytic tumors including diffuse astrocytic tumors produced weak immunoreactive bands, since podocalyxin is expressed in all vascular endothelial cells (Fig. 1).

Table 1
Results of podocalyxin immunostaining in 51 patients with astrocytic tumors

Tumor type	No. of cases	Podocalyxin				Positive rate
		+++	++	+	–	
Diffuse astrocytoma (grade II)	6	0	0	0	6	0%
Anaplastic astrocytoma (grade III)	14	0	1	5	8	42.9%
Glioblastoma (grade IV)	31	7	3	7	14	54.8%

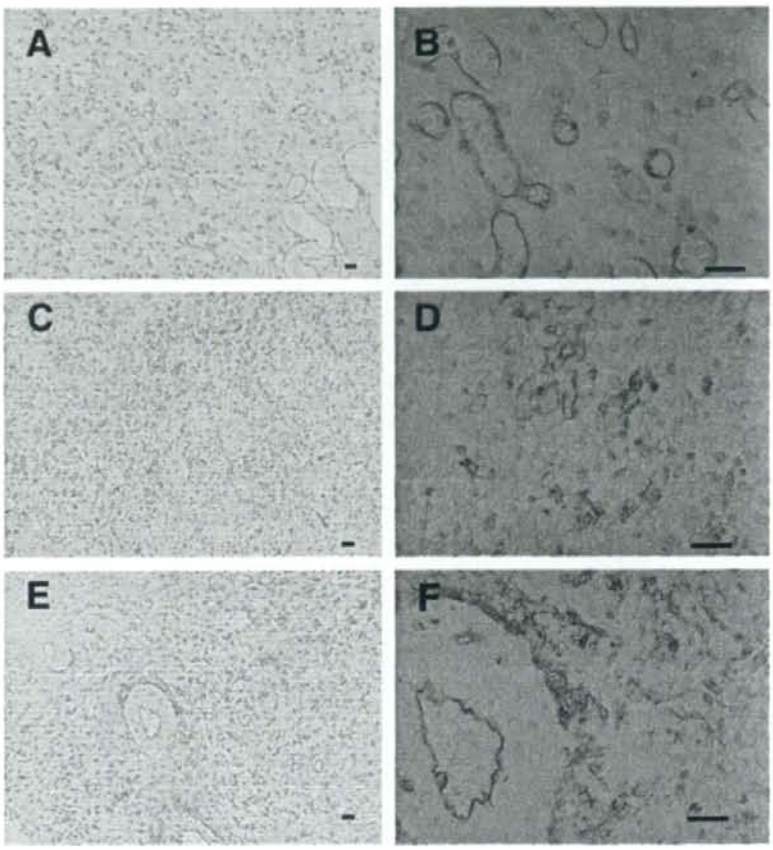

Fig. 1. Immunohistochemical detection of podocalyxin in astrocytic tumors. Podocalyxin was not detected on tumor cell surfaces in diffuse astrocytomas; however, podocalyxin staining was observed in vascular endothelial cells, although as shown in this figure few endothelial cells are usually detected in diffuse astrocytomas (A: 100×, B: 400×). In anaplastic astrocytoma, the tumor cell surface was stained positively (C: 100×, D: 400×). Accentuated staining is visible around an area of microvascular proliferation in glioblastoma (E: 100×, F: 400×). Bar, 10 μm.

Differential expression of the podocalyxin mRNA in astrocytic tumors

To quantify the expression of podocalyxin mRNA in human astrocytic tumors of different grades, we performed quantitative real-time PCR analyses of astrocytic tumors from 51 patients. The relative podocalyxin mRNA expression levels of each tumor grade are shown in Fig. 3. Average copy numbers of podocalyxin mRNA/μg total RNA in diffuse astrocytomas, anaplastic astrocytomas, and glioblastomas were 535 ± 289, 918 ± 595, and 3670 ± 2916, respectively. Podocalyxin transcript levels were significantly higher in glioblastomas than in diffuse astrocytomas or anaplastic astrocytomas ($p < 0.01$).

Discussion

Podocalyxin expression has been reported to increase the aggressive phenotype of breast and prostate cancer, and be correlated with their poor prognosis [10,14,17]. Recently, we showed that highly sulfated keratan sulfate detected by 5D4 antibody is upregulated in accordance with malignancy of astrocytic tumors [19]. We speculated that expression of core proteins of KS proteoglycan is upregulated in malignant astrocytic tumors. Podocalyxin was recently identified as a keratan sulfate (KS) proteoglycan: podocalyxin has the keratan sulfate antigens TRA-1-60 and TRA-1-81, which are also known as human pluripotent stem cell markers, in embryonal carcinoma [20]. Furthermore, podocalyxin expression correlates with tumor aggressiveness or malignancy; therefore, we herein investigated the podocalyxin expression in brain tumors, focusing on astrocytic tumors of different grades.

In this study, we first investigated the podocalyxin expression by immunohistochemistry (Fig. 1), and showed significantly different podocalyxin expression between anaplastic astrocytomas (Grade III; 42.9%) and glioblastoma (Grade IV; 54.8%; $p < 0.05$). Using Western blot analysis and real-time PCR, we confirmed this result (Figs. 2 and 3). Taken together, these results indicate that podocalyxin expression might be associated with the malignant progression of astrocytic tumors. We previously investigated the expression of podoplanin, another mucin-like sialoglycoprotein, which is associated with malignant progression of astrocytic tumors [21,24,25]. Podoplanin was detected on the cell surface in 27% of anaplastic astrocytomas and 47% of glioblastomas. In contrast, podoplanin expression was not observed in diffuse astrocytomas. Because both podocalyxin and podoplanin are associated with the malignancy of astrocytic tumors, we investigated whether podocalyxin expression is correlated with podoplanin; however, we found no correlation between the expression levels of the two sialoglycoproteins (data not shown). We might be able to predict the malignancy of astrocytic tumors if we appropriately combine

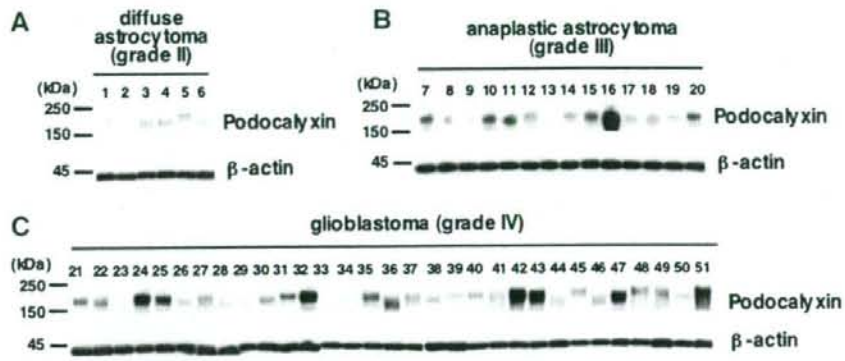

Fig. 2. Western blot analysis of podocalyxin expression in astrocytic tumors. Tissues from diffuse astrocytomas (A: lane 1–6), anaplastic astrocytomas (B: lane 7–20), and glioblastomas (C: lane 21–51) were solubilized, and 4 μg of the proteins were electrophoresed under reducing conditions on 10% polyacrylamide gel. The separated proteins were transferred to a PVDF membrane. After blocking with 3% skim milk in PBS, the membrane was incubated with anti-podocalyxin (upper panel) or anti-β-actin antibody (lower panel).

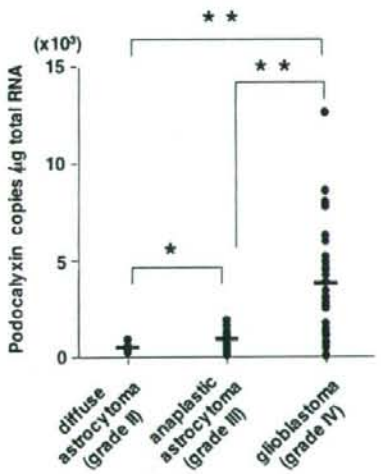

Fig. 3. Quantitative real-time PCR analysis of podocalyxin in astrocytic tumors. The transcript levels for a podocalyxin gene in 51 astrocytic tumors (six diffuse astrocytomas, 14 anaplastic astrocytomas, and 31 glioblastomas) were measured using real-time PCR. Values normalized to the level of total RNA are presented. $^{**}p < 0.01$, $^{*}p < 0.05$.

the expression level of these several molecules. Further study is needed to clarify the pathophysiological function of podocalyxin in astrocytic tumors, such as invasiveness or angiogenesis, using more clinical samples.

In summary, we investigated the expression of podocalyxin in 51 astrocytic tumors using immunohistochemistry, Western blot, and real-time PCR analyses. Podocalyxin expression was not observed in diffuse astrocytoma except in vascular endothelial cells. Furthermore, podocalyxin mRNA and protein expression were markedly higher in glioblastomas than in anaplastic astrocytomas. These data suggest that podocalyxin expression is associated with malignancy of astrocytic tumors, and might be useful as a prognostic factor.

Acknowledgments

This study was supported in part by Mitsubishi Pharma Research Foundation (Y. Kato), the YASUDA Medical Foundation (Y. Kato), the Toyama Foundation (Y. Kato), the Inoue Foundation for Science (Y. Kato), and Osaka Cancer Research Foundation (M.K. Kaneko).

References

[1] P. Kleihues, P.C. Burger, V.P. Collines, E.W. Newcomb, H. Ohagi, W.K. Cavenee, Astrocytic Tumors, Glioblastma, International Agency for Research on Cancer Press, Lyons, France, 2000. pp. 29–39.
[2] A. Giese, R. Bjerkvig, M.E. Berens, M. Westphal, Cost of migration: invasion of malignant gliomas and implications for treatment, J. Clin. Oncol. 21 (2003) 1624–1636.
[3] P. Kleihues, H. Ohgaki, Primary and secondary glioblastomas: from concept to clinical diagnosis, Neuro-oncology 1 (1999) 44–51.
[4] D. Kerjaschki, D.J. Sharkey, M.G. Farquhar, Identification and characterization of podocalyxin-the major sialoprotein of the renal glomerular epithelial cell, J. Cell Biol. 98 (1984) 1591–1596.
[5] J.E. Schnitzer, C.P. Shen, G.E. Palade, Lectin analysis of common glycoproteins detected on the surface of continuous microvascular endothelium in situ and in culture: identification of sialoglycoproteins, Eur. J. Cell Biol. 52 (1990) 241–251.
[6] T. Hara, Y. Nakano, M. Tanaka, K. Tamura, T. Sekiguchi, K. Minehata, N.G. Copeland, N.A. Jenkins, M. Okabe, H. Kogo, Y. Mukouyama, A. Miyajima, Identification of podocalyxin-like protein 1 as a novel cell surface marker for hemangioblasts in the murine aorta-gonad-mesonephros region, Immunity 11 (1999) 567–578.
[7] A. Miettinen, M.L. Solin, J. Reivinen, E. Juvonen, R. Vaisanen, H. Holthofer, Podocalyxin in rat platelets and megakaryocytes, Am. J. Pathol. 154 (1999) 813–822.
[8] R. Doyonnas, D.B. Kershaw, C. Duhme, H. Merkens, S. Chelliah, T. Graf, K.M. McNagny, Anuria, omphalocele, and perinatal lethality in mice lacking the CD34-related protein podocalyxin, J. Exp. Med. 194 (2001) 13–27.
[9] T. Takeda, W.Y. Go, R.A. Orlando, M.G. Farquhar, Expression of podocalyxin inhibits cell–cell adhesion and modifies junctional properties in Madin–Darby canine kidney cells, Mol. Biol. Cell 11 (2000) 3219–3232.
[10] A. Somasiri, J.S. Nielsen, N. Makretsov, M.L. McCoy, L. Prentice, C.B. Gilks, S.K. Chia, K.A. Gelmon, D.B. Kershaw, D.G. Huntsman, K.M. McNagny, C.D. Roskelley, Overexpression of the anti-adhesin podocalyxin is an independent predictor of breast cancer progression, Cancer Res. 64 (2004) 5068–5073.
[11] X. Chen, J. Higgins, S.T. Cheung, R. Li, V. Mason, K. Montgomery, S.T. Fan, M. van de Rijn, S. So, Novel endothelial cell markers in hepatocellular carcinoma, Mod. Pathol. 17 (2004) 1198–1210.
[12] J.T. Ney, H. Zhou, B. Sipos, R. Buttner, X. Chen, G. Kloppel, I. Gutgemann, Podocalyxin-like protein 1 expression is useful to differentiate pancreatic ductal adenocarcinomas from adenocarcinomas of the biliary and gastrointestinal tracts, Hum. Pathol. 38 (2007) 359–364.
[13] P. Stanhope-Baker, P.M. Kessler, W. Li, M.L. Agarwal, B.R. Williams, The Wilms tumor suppressor-1 target gene podocalyxin is transcriptionally repressed by p53, J. Biol. Chem. 279 (2004) 33575–33585.
[14] G. Casey, P.J. Neville, X. Liu, S.J. Plummer, M.S. Cicek, L.M. Krumroy, A.P. Curran, M.R. McGreevy, W.J. Catalona, E.A. Klein, J.S. Witte, Podocalyxin variants and risk of prostate cancer and tumor aggressiveness, Hum. Mol. Genet. 15 (2006) 735–741.
[15] W.M. Schopperle, D.B. Kershaw, W.C. DeWolf, Human embryonal carcinoma tumor antigen, Gp200/GCTM-2, is podocalyxin, Biochem. Biophys. Res. Commun. 300 (2003) 285–290.
[16] T.W. Kelley, D. Huntsman, K.M. McNagny, C.D. Roskelley, E.D. Hsi, Podocalyxin: a marker of blasts in acute leukemia, Am. J. Clin. Pathol. 124 (2005) 134–142.

[17] S. Sizemore, M. Cicek, N. Sizemore, K.P. Ng, G. Casey, Podocalyxin increases the aggressive phenotype of breast and prostate cancer cells in vitro through its interaction with ezrin, Cancer Res. 67 (2007) 6183–6191.
[18] N. Hayatsu, S. Ogasawara, M.K. Kaneko, Y. Kato, H. Narimatsu, Expression of highly sulfated keratan sulfate synthesized in human glioblastoma cells, Biochem. Biophys. Res. Commun. 368 (2008) 217–222.
[19] Y. Kato, N. Hayatsu, M.K. Kaneko, S. Ogasawara, T. Hamano, S. Takahashi, R. Nishikawa, M. Matsutani, K. Mishima, H. Narimatsu, Increased expression of highly sulfated keratan sulfate synthesized in malignant astrocytic tumors, Biochem. Biophys. Res. Commun. 369 (2008) 1041–1046.
[20] W.M. Schopperle, W.C. DeWolf, The TRA-1-60 and TRA-1-81 human pluripotent stem cell markers are expressed on podocalyxin in embryonal carcinoma, Stem Cells 25 (2007) 723–730.
[21] K. Mishima, Y. Kato, M.K. Kaneko, R. Nishikawa, T. Hirose, M. Matsutani, Increased expression of podoplanin in malignant astrocytic tumors as a novel molecular marker of malignant progression, Acta Neuropathol. (Berlin) 111 (2006) 483–488.
[22] J. Achenbach, M. Mengel, I. Tossidou, I. Peters, J. K. Park, M. Haubitz, J. H. Ehrich, H. Haller, M. Schiffer, Parietal epithelia cells in the urine as a marker of disease activity in glomerular diseases, Nephrol. Dial. Transpl., in press.
[23] A.B. Choo, H.L. Tan, S.N. Ang, W.J. Fong, A. Chin, J. Lo, L. Zheng, H. Hentze, R.J. Philp, S.K. Oh, M. Yap, Selection against undifferentiated human embryonic stem cells by a cytotoxic antibody recognizing podocalyxin-like protein-1, Stem Cells 26 (2008) 1454–1463.
[24] Y. Kato, M.K. Kaneko, A. Kunita, H. Ito, A. Kameyama, S. Ogasawara, N. Matsuura, Y. Hasegawa, K. Suzuki-Inoue, O. Inoue, Y. Ozaki, H. Narimatsu, Molecular analysis of the pathophysiological binding of the platelet aggregation-inducing factor podoplanin to the C-type lectin-like receptor CLEC-2, Cancer Sci. 99 (2008) 54–61.
[25] Y. Kato, M.K. Kaneko, A. Kuno, N. Uchiyama, K. Amano, Y. Chiba, Y. Hasegawa, J. Hirabayashi, H. Narimatsu, K. Mishima, M. Osawa, Inhibition of tumor cell-induced platelet aggregation using a novel anti-podoplanin antibody reacting with its platelet-aggregation-stimulating domain, Biochem. Biophys. Res. Commun. 349 (2006) 1301–1307.

Diffuse large B-cell lymphoma after transformation from low-grade follicular lymphoma: morphological, immunohistochemical, and FISH analyses

Akiko Miyagi Maeshima,[1,4] Mutsuko Omatsu,[1] Junko Nomoto,[2] Dai Maruyama,[2] Sung-Won Kim,[2] Takashi Watanabe,[2] Yukio Kobayashi,[2] Kensei Tobinai[2] and Yoshihiro Matsuno[3]

[1]Clinical Laboratory and [2]Hematology and Stem Cell Transplantation Divisions, National Cancer Center Hospital, Tsukiji 5-1-1, Chuo-ku, Tokyo 104-0045, and [3]Department of Surgical Pathology, Hokkaido University Hospital, Kita 14 Nishi 5, Kita-ku, Sapporo 060-8648, Japan

(Received March 12, 2008/Revised April 27, 2008/Accepted May 6, 2008/Online publication June 28, 2008)

Follicular lymphoma (FL) is one of the most common subtypes of non-Hodgkin lymphoma and frequently transforms to diffuse large B-cell lymphoma (DLBCL). To clarify some aspects of the natural history of FL, we retrospectively examined 43 consecutive patients who had DLBCL with pre- or coexisting FL grade 1 or 2. The patients comprised 22 men and 21 women with a median age of 53 years. Most of the patients (34/43) showed advanced-stage (III or IV) disease initially. We examined both FL and DLBCL components morphologically, immunohistochemically, and by interface fluorescence *in situ* hybridization (FISH: IGH/BCL2 fusion, *BCL6 translocation*) analysis. Most of the DLBCLs were classified as the centroblastic subtype, with two exceptions of the anaplastic subtype. Immunohistochemical analysis of both the FL and DLBCL components revealed the following respective positivity rates: CD20 100%/100%, CD10 86%/66%, Bcl-2 96%/91%, Bcl-6 84%/88%, MUM1 16%/34%, CD30 0%/20%, CD138 0%/0%, and CD5 0%/3%. Loss of CD10 (*6/36, 17%*) and gain of MUM1 (*7/28, 25%*) and CD30 (*5/21, 24%*) through transformation were not infrequent. High positivity rates for Bcl-2 and Bcl-6 were maintained throughout transformation. Among the DLBCLs, 84% were classified as the germinal center B-cell phenotype (GCB) and 16% as non-GCB in accordance with the criteria of Hans *et al.* IGH/BCL2 fusion was detected by FISH in 89% of FLs and 82% of DLBCLs. BCL6 translocation was detected in 1/6 (17%) DLBCLs without IGH/BCL2 fusion. Thus, although the morphological features and FISH results for DLBCL were consistent with transformed FL, the immunophenotype showed wide heterogeneity. (*Cancer Sci* 2008; 99: 1760–1768)

Follicular lymphoma (FL) is one of the most common subtypes of non-Hodgkin lymphoma in the Western world, accounting for 22% of all cases worldwide.[1] FL occurs over a broad range of ages, and most cases are manifested initially in lymph nodes.

The risk of FL transformation has been reported as being approximately 20% at 8 years.[2,3] Transformation to DLBCL is observed frequently, with cells most commonly resembling centroblasts,[4] but occasionally resembling anaplastic large cells with CD30 expression.[5] Rare cases have transformed to Burkitt or Burkitt-like lymphoma,[6] or precursor B-lymphoblastic lymphoma/acute lymphoid leukemia.[7] Moreover, composite FL and Hodgkin lymphoma have been suggested to represent two morphologic manifestations of the same tumor clones.[8,9]

In recent years, several analyses of genetic alterations that appear to affect the risk for FL transformation have been reported, including c-MYC translocation,[6] p53 mutation,[10,11] deletions of the tumor suppressor genes p15 and p16,[12,13] and chromosomal 6q23-26 and 17q aberrations.[14] However, there have been few immunohistochemical analyses of transformed FL. FL is positive for the pan-B-cell marker CD20, and frequently positive for CD10, Bcl-2 and Bcl-6, but is usually negative for the postgerminal center B-cell or plasma cell markers CD30, MUM1 and CD138, and CD5. Because only one study has demonstrated gain of CD30 expression through FL transformation,[5] we considered that more analyses were needed to clarify the immunophenotypic changes occurring during the transformation of FL to DLBCL.

Since 2000 DLBCL has been subdivided into GCB and non-GCB (including the activated B-cell phenotype [ABC] and type 3 phenotype) using the cDNA microarray technique.[15,16] The GCB group shows better outcomes and includes cases with translocation (14;18)(q32;q21). For clinical practice, Hans *et al.* showed that a panel of immunohistochemical markers comprising CD10, Bcl-6, and MUM1 could be used on paraffin-embedded tissues to separate DLBCL into tumors with a GCB or non-GCB phenotype.[17] Davies *et al.* examined 35 cases of transformed FL, and found that 89% of them had a GCB phenotype and 9% had a non-GCB phenotype.[18]

The translocation (14;18)(q32;q21) is present in 80–100% of FLs in Western countries,[19,20] whereas in South-East Asia, including Japan, the incidence of translocation is considerably lower: about 60%.[21] It is unclear whether FL with t(14;18) frequently transforms to DLBCL.

The aim of this study was to clarify the natural history of FL, mainly in view of immunophenotypic changes through transformations. We evaluated low-grade FLs and their transformant DLBCLs using morphological, immunhistochemical, and FISH analyses to delineate the heterogeneity of DLBCL after transformation from low-grade FL.

Materials and Methods

Patients. The criteria used for identification of transformed FL were those reported for aggressive B-cell lymphomas in a review based on the workshop of the XIth Meeting of the European Association for Haematopathology.[22] Briefly, it was considered that the term 'transformation' should be used only when there was morphological evidence of simultaneous or prior low-grade FL. Therefore, in the present study, we chose DLBCL with simultaneous or prior low-grade (grade 1 or 2) FL. We retrospectively studied 43 consecutive patients with DLBCL with pre- (20 cases) or coexisting (23 cases) FL grade 1 or 2 treated at the National Cancer Center Hospital, Tokyo, Japan, between 1997 and 2005. The total number of DLBCL specimens was 47 (1–3 per case), and the total number of specimens of low-grade FL was 53 (1–5 per case). A total of 400 FLs and 653 DLBCLs were registered during the same

*To whom correspondence should be addressed. E-mail: akmaeshi@ncc.go.jp

doi: 10.1111/j.1349-7006.2008.00873.x

period. Clinical information was extracted from the medical records, and is summarized in Table 1.

Morphological review. The materials were fixed in 10% neutral-buffered formalin, embedded in paraffin, cut into 4-μm thick sections, and stained with hematoxylin–eosin (HE) for histologic evaluation. All specimens were reviewed by two pathologists (AMM and YM) to confirm that the morphologic characteristics fulfillled the criteria for FL and DLBCL in the 2001 World Health Organization classification of lymphoid neoplasms.[23] Tumors were judged to be FL grade 1 when neoplastic follicles contained 0–5 centroblasts/10 HPF, and FL grade 2 when they contained 6–15 centroblasts/10 HPF. We diagnosed DLBCL when the tumor cells were spread diffusely without a follicular pattern and large lymphoid cells accounted for more than 30% of the tumor cells. DLBCL was subclassified as the centroblastic, anaplastic, immunoblastic, or T-cell/histiocyte rich variant. The centroblastic variant was subclassified as monomorphous (comprising only large lymphoid cells) or polymorphous (comprising a mixture of large- and medium-sized lymphoid cells).

Immunohistochemistry and *in situ* hybridization. We performed immunohistochemical staining for both FL and DLBCL components on formalin-fixed paraffin-embedded tissues using a panel of monoclonal and polyclonal antibodies. Sections 4-μm thick were cut from each paraffin block, deparaffinized, and incubated at 121°C in pH 6.0 citrate buffer for 10 min for antigen retrieval. Antibodies included those against the following antigens: a pan-B-cell marker, CD20 (L26, ×100; Dako, Glostrup, Denmark); a pan-T-cell marker, CD3 (PS1, ×25; Novocastra, Newcastle-upon-Tyne, UK); FL markers, CD10 (56C6, ×50; Novocastra), Bcl-2 (124, ×100; Dako); and Bcl-6 (poly, ×50; Dako, Kyoto, Japan); postgerminal center B-cell or plasma cell markers, CD30 (Ber-H2, ×100; Dako, Denmark); MUM1 (MUM1p, ×50; Dako, Japan); and CD138 (5F7, ×25; Novocastra); and CD5 (4C7, ×50; Novocastra), employing an autostainer with the standard polymer (Dako autostainer plus: CD3, CD5, CD10, and CD30) or labeled streptavidin-biotin method (Biogenex autostainer: CD20 and Bcl-2), or manually by the standard avidin-biotin complex method (Bcl-6, MUM1, and CD138). Immunoreactivity was judged positive if more than 30% of the tumor cells were stained. All immunohistochemical specimens were judged by AM Maeshima, and Y Matsuno confirmed them.

To classify each case as having either a 'GCB phenotype' or a 'non-GCB phenotype', a panel of three antigens (CD10, Bcl-6, MUM1) was used according to the protocol reported by Hans *et al.*[17] Briefly, cases were assigned to the 'GCB phenotype' if the specimens were positive for CD10. If the specimens were negative for both Bcl-6 and CD10, the corresponding cases were assigned to the 'non-GCB phenotype'. If the specimens were positive for Bcl-6 and negative for CD10, the expression of MUM1 was used to determine the group: if MUM1 was negative, the case was assigned to the 'GCB phenotype', and if positive, to the 'non-GCB phenotype'.

Interphase fluorescence *in situ* hybridization (FISH) analysis. Sections 4-μm thick were cut from each paraffin block and used for FISH analysis. The specimens were treated with a 2× saline sodium citrate buffer (SSC, pH 7.3), digested with 0.005% and 0.3% pepsin/0.01 N HCl for 14 min at 37°C, rinsed in 1× phosphate buffer saline (PBS, pH 7.4) for 5 min, formalin $MgCl_2$/PBS for 10 min, rinsed in 1× PBS for 5 min twice, and dehydrated in an ethanol series. Next, the samples were denatured in 70% formamide/20× SSC for 2 min at 37°C and dehydrated with 70% ethanol for 5 min, followed by 100% ethanol. Denatured probes (10 μL) were dropped onto the slides, covered with a coverslip, and sealed with rubber cement. The slides were then treated using a microwave procedure to intensify the signals. The microwave (MI-77; Azumaya Company, Tokyo, Japan) was set to irradiate the samples for 3-second periods at intervals of 2 s, for a total of 60 min at a frequency of 2.45 GHz and an output power of 250 W with the temperature sensor set to 37°C. After incubation overnight at 37°C, the slides were washed with 50% formamide/2× SSC for 10 min at 45°C, and then washed twice more for 10 min each at room temperature; the slides were then washed with 2× SSC for 10 min. The specimens were rinsed in 4× SSC/0.05% Triton for 5 min, 2× SSC for 5 min at 45°C, and 0.2× SSC at room temperature. The slides were covered with antifade solution and viewed under a BX60 fluorescence microscope (Olympus, Tokyo, Japan) using a 100× oil immersion lens and appropriate filters.

LSI IGH Spectrum Green/LSI BCL2 Spectrum Orange Dual Fusion Translocation Probe (Vysis, Downers Grove, IL, USA) was used to detect t(14;18): IGH/BCL2 fusion. LSI BCL6 Dual Color, Break Apart Rearrangement Probe (Vysis) was used to detect 3q27: BCL6 translocation. Judgment of the fusion gene was performed as described previously.[21] Briefly, a total of 50–200 nuclei per case were scored, and if more than 2% of the tumor cells had two fusion signals in the IGH/BCL2 examination, they were judged positive for fusion. If more than 1.5% of tumor cells had split signals in the BCL6 examination, they were judged positive for translocation.

Statistical analysis. Five-year and 10-year overall survival rates were calculated by the Kaplan–Meier method. Univariate analysis was performed using the log-rank test for clinicopathologic parameters, as shown in Tables 1–3. Clinical information of patients with pre-existing FL and those with coexisting FL was compared by the Fisher's exact test, Mann–Whitney *U*-test or log-rank test in Table 2. Differences were considered significant when *P*-value was less than 0.05.

Results

Patients. Clinical information is summarized in Table 1. The patients comprised 22 men and 21 women, ranging in age from 25 to 80 years with a median age of 53 years. Most of them (34/43) had advanced-stage (III or IV) initially. All of the patients received treatments after initial diagnoses: cyclophosphamide, doxorubicin, vincristine and prednisone (CHOP) ± radiation (12 cases), rituximab (R)-CHOP ± radiation (22 cases), or other types of treatment (cyclophosphamide, vincristine, prednisone and procarbazine (C-MOPP), vincristine, cyclophosphamide, prednisone and doxorubicin (VEPA), methotrexate, doxorubicin, cyclophosphamide, vincristine, prednisone and bleomycin (MACOP-B), vincristine/vindesine, doxorubicin and prednisone (VCR/VDS + DOX + PSL), R+ radiation and radiation) (8 cases). Overall survival after initial diagnosis was 76.5% at 5 years and 57.3% at 10 years. Overall survival after transformation was 60.0% at 5 years. Clinical information was compared between 19 patients with pre-existing FL and 24 patients with coexisting FL, and is summarized in Table 2.

Morphology. The results of morphological analysis, immunohistochemical staining for each antibody, and FISH analysis are summarized in Table 3 and Table 4. A total of 47 DLBCL specimens from 43 patients were reviewed. The biopsy sites were lymph node (27), tonsil (6), spleen (1), and extranodal sites (13: gingiva 1, stomach 1, small intestine 1, terminal ileum 1, rectum 3, bone marrow 2, skin 3, lung 1). The subtypes of DLBCL in the final specimens were centroblastic monomorphous (30), centroblastic polymorphous (11), and anaplastic (2). Notably, one case (no. 38) finally transformed to classical Hodgkin lymphoma, mixed cellularity, after transformation of FL to DLBCL. Massive necrosis was detected in four cases (9%).

A total of 53 FL specimens from 43 patients were reviewed. The biopsy sites were lymph node (21), tonsil (2), spleen (1), and extranodal sites (29: nasopharynx 1, esophagus 1, stomach 6, duodenum 6, small intestine 2, colon 1, bone marrow 11, skin 1). The grades of FL were grade 1 (20), grade 2 (27), judged as limited to low-grade FL due to the very small amount

Table 1. Patient characteristics

Case	Age/ gender	Stage	IPI	Initial diagnosis (site)	Initial therapy /response	Interval to transformation in months (time of relapse)	Second diagnosis (site)	Subtype of DLBCL	Follow-up months	Outcome from initial diagnosis
1	50/F	2	L	DLBCL + FL, gr.3a + FL, gr.1 (spleen)	Rx3 + CHOPx7/CR	0		anaplastic	40	AWD
2	47/M	2	L	FL, gr.2 (LN)	CHOPx8/CR	91 (2nd)	DLBCL (tonsil)	centroblastic	96	AWD
3	77/M	3	HI	FL, gr.1 (LN)	VCR/VDS, DOX, PSL/unknown	24 (1st)	DLBCL (LN)	centroblastic	31	DOD
4	45/M	3	L	FL, gr.1 (LN)	C-MOPPx11/CR	71 (4th)	DLBCL + FL, gr.3a (LN)	centroblastic	71	AWD
5	44/M	3	L	FL, gr.2 (LN, BM)	R-CHOPx6/PR	69 (1st)	DLBCL + FL, gr.2 (BM)	centroblastic	69	AWD
6	40/F	4	LI	FL, gr.1 (LN)	R-CHOPx6/CR	38 (2nd)	DLBCL + FL, gr.3a (tonsil), DLBCL (rectum), DLBCL (small intestine)	centroblastic	69	AWD
7	66/F	4	LI	FL, gr.1 (LN)	CHOPx3/PR	11 (1st)	DLBCL + FL, gr.3a (LN), DLBCL (skin)	centroblastic	66	AWD
8	80/F	3	HI	DLBCL + FL, gr.3a + FL, gr.2 (LN)	CHOPx5/PR	0		centroblastic	46	DOD
9	51/F	1	L	FL, gr.2 (duodenum)	radiation 40Gy/CR	10 (1st)	DLBCL (LN)	centroblastic	71	AWOD
10	67/M	3	LI	FL, gr.2 (LN)	VEPAx14/CR	93 (1st)	DLBCL (tonsil)	centroblastic	101	DOD
11	60/M	4	LI	DLBCL + FL, gr.2 (small intestine)	CHOPx8 + radiation 39Gy/CR	0		centroblastic	59	AWOD
12	25/F	4	LI	FL, gr.1 (duodenum), DLBCL + FL, gr.3a (LN)	Rx4 + CHOPx8/CR	0		centroblastic	69	AWOD
13	53/M	4	HI	DLBCL + FL, gr.2 (skin)	CHOPx8/PR	0		centroblastic	23	AWD
14	49/M	4	LI	FL, gr.2 (BM)	MACOP–Bx4/PR	49 (2nd)	DLBCL (skin)	centroblastic	55	DOD
15	61/F	3	HI	DLBCL + FL, gr.2 (LN)	Rx4 + CHOPx8/CR	0		centroblastic	44	AWOD
16	46/M	2	L	DLBCL + FL, gr.3a + FL, gr.2 (LN)	R-CHOPx8 + radiation 40Gy/PD	0		centroblastic	19	DOD
17	66/F	3	HI	DLBCL + FL, gr.3a + FL, gr.2 (LN)	CHOPx2 + radiation 40Gy/CR	0		centroblastic	43	AWOD
18	43/M	2	L	DLBCL + FL, gr.1 (LN)	R-CHOPx6 + radiation 40Gy/CR	0		centroblastic	72	AWOD
19	60/F	3	LI	FL, gr.1 (LN, duodenum)	CHOPx8/CR	40 (1st)	DLBCL (tonsil)	centroblastic	80	AWOD
20	41/F	4	LI	FL, gr.2 (tonsil), DLBCL (LN)	R-CHOPx8 + radiation 40Gy/CR	0		centroblastic	38	AWOD
21	72/F	2	LI	FL, gr.2 (LN)	R-CHOPx8 + radiation 40Gy/PR	84 (1st)	DLBCL (LN)	centroblastic	116	AWD
22	46/F	4	H	FL, gr.2 (duodenum, stomach), DLBCL (LN)	R-CHOPx8 + radiation 40Gy/CR	0		centroblastic	32	AWD
23	44/M	3	L	DLBCL + FL, gr.2 (LN)	R-CHOPx8/CR	0		centroblastic	30	AWOD
24	53/F	4	LI	FL, gr.2 (LN)	R + radiation 39Gy/CR	29 (1st)	DLBCL (lung)	centroblastic	29	AWD
25	53/F	4	HI	FL, gr.1 (duodenum, stomach, BM, colon, tonsil), DLBCL + FL, gr.3a (tonsil)	R-CHOPx5/CR	0		centroblastic	33	AWD
26	42/F	4	L	DLBCL + FL, gr.3a (LN), FL, gr.1 (BM)	R-CHOPx6/CR	0		centroblastic	24	AWOD
27	54/M	4	L	FL, gr.2 (LN, BM)	CHOPx8/PR	49 (1st)	DLBCL + FL, gr.3a (BM)	centroblastic	49	AWD

doi: 10.1111/j.1349-7006.2008.00873.x

Table 1. *Continued*

Case	Age/ gender	Stage	IPI	Initial diagnosis (site)	Initial therapy /response	Interval to transformation in months (time of relapse)	Second diagnosis (site)	Subtype of DLBCL	Follow-up months	Outcome from initial diagnosis
28	54/M	4	H	DLBCL + FL, gr.3b + FL, gr.2 (LN)	R-CHOPx8/PR	0		centroblastic	16	AWOD
29	47/M	3	LI	FL, gr.1 (BM)	CHOPx6/CR	46 (2nd)	DLBCL + FL, gr.3b (LN)	centroblastic	47	AWOD
30	59/M	3	L	FL, gr.1 (duodenum), DLBCL + FL, gr.3a (LN)	R-CHOPx6/CR	0		centroblastic	20	AWOD
31	52/M	3	L	DLBCL + FL, gr.3a + FL, gr.2 (LN)	R-CHOPx5/CR	0		centroblastic	18	AWOD
32	57/M	4	L	FL, gr.2 (BM)	R-CHOPx6/CR	26 (1st)	DLBCL + FL, gr.3a (LN)	anaplastic	27	AWD
33	47/F	3	L	DLBCL + FL, gr.1 (LN)	CHOPx6/CR	0		centroblastic	38	AWD
34	47/M	4	LI	FL, low grade (BM), DLBCL (LN)	R-CHOPx8/PR	0		centroblastic	13	AWD
35	47/F	4	L	FL, gr.2 (stomach, BM), DLBCL + FL, gr.3a (LN)	R-CHOPx8/CR	0		centroblastic	7	AWOD
36	59/F	1	L	FL, gr.1 (LN)	CHOPx3 + radiation/CR	24 (1st)	DLBCL (LN)	centroblastic	24	AWD
37	54/M	4	L	FL, low grade (BM), DLBCL + FL, gr.3b (LN)	R-CHOPx6/CR	0		centroblastic	12	AWOD
38	61/F	4	H	FL, low grade (esophagus, stomach), DLBCL + FL, gr.3a (LN), DLBCL (terminal ileum, rectum)	R-CHOPx8/NC	0	HL, MC (LN)	centroblastic	28	DOD
39	68/M	1	L	FL, low grade (BM), DLBCL + FL, gr.3a (LN)	CHOPx3 + radiation/CR	0		centroblastic	8	AWOD
40	79/M	1	L	FL, gr.2 (nasopharynx)	radiation 40Gy/CR	54 (2nd)	DLBCL (stomach)	centroblastic	152	DOD
41	70/M	4	HI	FL, gr.1 (stomach)	Rx4 + CHOPx6/NC	37 (1st)	DLBCL (gingival)	centroblastic	133	DOD
42	45/F	4	L	FL, gr.2 (LN)	C–MOPPx7/CR	21 (1st)	DLBCL (rectum)	centroblastic	37	DOD
43	56/F	4	LI	FL, low grade (stomach), DLBCL (tonsil)	unknown	0		centroblastic	0	unknown

AWD, alive with disease; AWOD, alive without disease; CHOP, cyclophosphamide, doxorubicin, vincristine and prednisone; C-MOPP, cyclophosphamide, vincristine, prednisone and procarbazine; CR, complete remission; DLBCL, diffuse large B-cell lymphoma; DOD, dead of disease; FL, follicular lymphoma; gr. grade; H, high; HI, high intermediate; HL, MC, Hodgkin lymphoma, mixed cellularity; IPI, international prognostic index; L, low; LI, low intermediate; MACOP-B, methotrexate, doxorubicin, cyclophosphamide, vincristine, prednisone and bleomycin; NC, no change; PD, progressive disease; PR, partial remission; R, rituximab; VCR/VDS + DOX + PSL, vincristine/vindesine, doxorubicin and prednisone; VEPA, vincristine, cyclophosphamide, prednisone and doxorubicin.

Table 2. Patients' clinical data at initial diagnosis

	19 cases with pre-existing FL	24 cases with coexisting FL	*P*-value[†]
Gender (male/female)	11/8	11/13	0.54
Age (median, range)	57 (40–79)	52 (25–80)	0.30
Stage (I, II/III, IV)	5/14	4/20	0.47
LDH (normal/higher than normal)	13/6	14/10	0.54
PS (0/≥1)[‡]	13/2	13/7	0.24
Extranodal involvement (0/≥1)	13/6	11/13	0.21
B symptom (–/+)[‡]	14/1	18/2	0.72
Bulky mass (–/+)	18/1	21/3	0.62
IPI (L, LI/HI, H)[‡]	14/1	14/6	0.10
5-year OS from initial diagnosis	80.2%	65.2%	0.43
5-year OS from transformation	47.7%	65.2%	0.11

[†]Fisher's exact test, Mann–Whitney *U*-test or log-rank test.
[‡]data for PS, B symptom, and IPI were not obtained in eight cases.
FL, follicular lymphoma; H, high; HI, high intermediate; IPI, international prognostic index; L, low; LDH, serum lactate dehydrogenase; LI, low intermediate; OS, overall survival; PS, performance status.

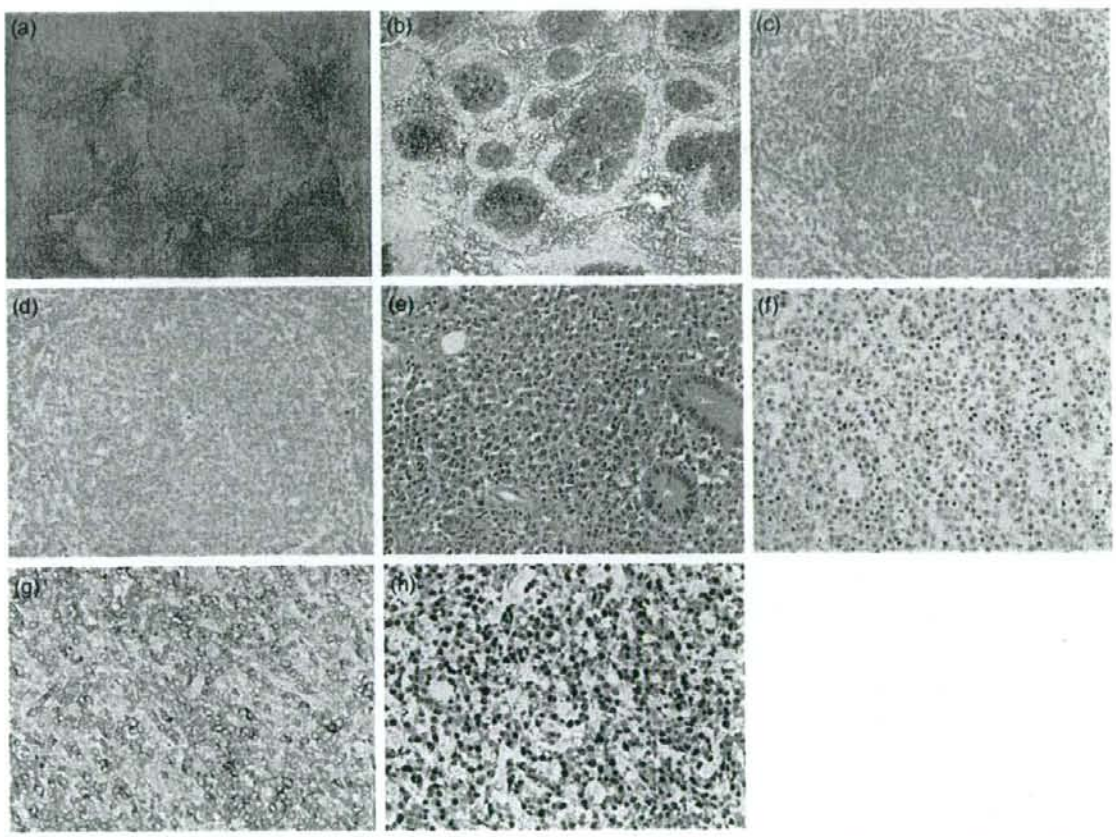

Fig. 1. (a–h) A case of transformation of follicular lymphoma (FL) with a CD10⁺/CD30⁻/MUM1⁻ phenotype to diffuse large B-cell lymphoma (DLBCL) with a CD10⁻/CD30⁺/MUM1⁺ phenotype. FL, lymph node. (a) Hematoxylin–eosin (HE) (×40), (b) CD10⁺ (×40), (c) CD30⁻ (×200), (d) MUM1– (×200). DLBCL, small intestine, (e) HE (×400), (f) CD10⁻ (×200), (g) CD30⁺ (×200), (h) MUM1⁺ (×200).

of material available (6). There were 17 cases with a grade 3a component and three with a grade 3b component.

Immunohistochemistry. The results of immunohistochemistry are summarized in Table 3, Table 4, and Fig. 1. Paraffin sections were available for 41 FL specimens and 43 DLBCL specimens, but in relatively few of the FL and/or DLBCL cases were not available for some of the markers. All tumors were positive for CD20 and negative for CD3. CD10 was positive in 86% (31/36)

doi: 10.1111/j.1349-7006.2008.00873.x

Table 3. Results of immunohistochemistry and FISH analysis

Case no.	Immunophenotype of a low-grade (grade 1 or 2) FL component								FISH[†]		Immunophenotype of a DLBCL component[‡]								FISH		
	CD20	CD10	Bcl-2	Bcl-6	MUM1	CD30	CD5	CD138	IGH/BCL2	BCL6 translocation	CD20	CD10	Bcl-2	Bcl-6	MUM1	CD30	CD5	CD138	GC/non-GC	IGH/BCL2	BCL6 translocation
1	+	+	+	+	−	−	−	−	+		+	+	+	+	−	−	nt	−	GC	+	
2	+	+	+	−	−	nt	−	−	+		+	+	+	+	+	+	+	−	GC	+	
3	+	+	+	+	−	−	nt	−	nt		+	+	+	+	+	−	−	−	GC	+	
4	nt	nt	nt	nt	nt	nt	nt	nt	nt		+	+	+	+	−	−	−	−	GC	+	
5	+	+	+	+	−	−	nt	−	nt		+	nt	+	+	−	−	−	−	GC	nt	
6	+	+	+	+	−	−	−	−	+		+	−	+	−	+	+	−	−	nonGC	+	
7	+	+	+	+	−	−	nt	−	nt		+	−	+	+	+	−	−	−	nonGC	+	
8	+	+	+	+	−	nt	nt	−	+		+	+	+	+	−	−	−	−	GC	+	
9	+	+	+	+	−	−	−	−	+		+	−	nt	nt	nt	nt	nt	nt		+	
10	+	+	+	nt	nt	nt	nt	nt	nt		+	+	−	+	−	−	−	−	GC	+	
11	+	+	+	−	−	−	−	−	nt		+	+	+	−	−	−	−	−	GC	nt	
12	+	+	+	+	+	−	−	−	nt		+	+	+	+	+	−	−	−	GC	−	−
13	+	+	+	+	−	−	nt	−	+		+	+	+	+	−	−	−	−	GC	+	
14	+	nt	+	−	−	−	nt	−	nt		+	+	+	+	−	−	−	−	GC	+	
15	+	+	+	+	−	−	nt	−	+		+	+	+	+	−	nt	−	−	GC	+	
16	+	+	+	+	+	nt	−	nt	+		+	+	+	+	−	nt	−	nt	GC	+	
17	nt	nt	nt	nt	nt	nt	nt	nt	nt		+	+	+	nt	nt	nt	−	nt	GC	nt	
18	+	−	+	+	−	nt	−	nt	nt		+	−	+	+	+	nt	−	nt	nonGC	nt	
19	+	+	+	+	−	−	−	−	nt		+	−	+	nt	nt	nt	nt	nt		nt	
20	+	+	+	+	−	−	nt	−	nt		+	+	+	+	+	−	−	−	GC	+	
21	+	−	−	nt	nt	nt	nt	nt	−	nt	+	−	+	+	−	−	−	−	GC	−	
22	+	+	+	+	−	−	−	−	nt		+	+	+	+	−	−	−	−	GC	+	
23	+	−	+	+	−	−	nt	−	+		+	−	+	nt	nt	nt	−	nt		+	
24	+	+	+	+	−	−	−	−	nt		+	−	+	+	+	+	−	−	nonGC	+	
25	+	+	+	−	+	−	−	−	+		+	+	+	+	+	−	−	−	GC	+	
26	+	+	+	−	−	−	nt	−	+		+	+	+	+	−	nt	nt	nt	GC	+	
27	+	+	+	+	−	nt	nt	nt	+		+	nt	−	+	−	−	−	−	GC	+	
28	+	+	+	nt	nt	nt	nt	nt	+		+	+	+	nt	nt	nt	−	nt	GC	+	
29	+	nt	+	+	+	−	−	−	nt		+	−	+	+	+	+	−	−	nonGC	−	−
30	+	+	+	nt	nt	nt	−	nt	+		+	+	+	+	−	−	−	−	GC	+	
31	+	−	+	nt	nt	nt	nt	nt	nt		+	−	+	nt	−	nt	nt	nt		nt	
32	nt	nt	+	+	+	−	nt	−	nt		+	−	+	nt	+	+	−	nt	nonGC	+	
33	+	+	+	nt	nt	nt	−	nt	nt		+	+	+	nt	nt	−	−	nt	GC	nt	
34	+	+	−,+	+	−	−	−	−	nt		+	+	+	nt	−	nt	−	nt	GC	+	
35	+	+	+	+	−	−	−	−	nt		+	+	+	+	−	−	−	−	GC	+	
36	+	+	+	+	−	−	−	−	nt		+	+	−	+	−	−	−	−	GC	−	−
37	+	nt	+	nt	nt	−	nt	nt	−	nt	+	−	−	nt	nt	nt	−	nt		nt	
38	+	+	+	nt	nt	nt	−	nt	+		+	+	+	−	+	−	−	−	GC	+	
39	+	nt	+	nt	nt	−	nt	nt	nt		+	−	+	+	−	+	−	−	GC	−	+
40	+	+	+	+	−	−	nt	−	nt		+	+	+	−	−	−	−	−	GC	−	−
41	+	+	+	+	−	−	nt	−	nt		+	+	+	+	−	−	−	−	GC	+	
42	+	+	+	+	−	−	−	−	nt		+	−	+	+	−	−	−	nt	GC	nt	
43	+	−	+	nt	nt	nt	−	nt	+		+	+	+	nt	nt	nt	−	nt	GC	+	

[†]judged from the final biopsy specimen, [‡]fluorescence *in situ* hybridization for IGH/BCL2 fusion.
DLBCL, diffuse large B-cell lymphoma; FISH, fluorescence *in situ* hybridization; FL, follicular lymphoma; GC, germinal center B-cell phenotype; nt, not tested.

Table 4. Summary of results of immunohistochemistry and FISH analysis

Antibody	FL component	DLBCL component	Gain/loss/no change
CD20	100% (40/40)	100% (43/43)	
CD10	86% (31/36)*	66% (27/41)†	1/6/29
Bcl-2	96% (42/44)	91% (38/42)	1/4/37
Bcl-6	84% (26/31)	88% (28/32)	4/2/20
MUM1	16% (5/31)	34% (12/35)	7/1/20
CD30	0% (0/28)	20% (6/30)	5/0/16
CD138	0% (0/28)	0% (0/28)	
CD5	0% (0/21)	3% (1/38)	1/0/19
GCB, non-GCB		84% (31/37), 16% (6/37)	
FISH: IGH/BCL2	89% (16/18)	82% (28/34)	

†excluding bone marrow specimens.
DLBCL, diffuse large B-cell lymphoma; FISH, fluorescence *in situ* hybridization; FL, follicular lymphoma; GCB, germinal center B-cell phenotype.

of FLs and 66% (27/41) of DLBCLs, representing a gain in one case, loss in six cases, and no change in 29 cases (including 21 positive cases and eight negative cases). Bone marrow specimens were excluded because only these materials showed extremely low CD10 expression. Among six cases of DLBCL showing loss of CD10, two were diagnosed as DLBCL several times (nos. 6 and 7), and both cases showed loss of CD10 expression between the first and second occasions. Bcl-2 and Bcl-6 were frequently expressed in both FL and DLBCL. Bcl-2 was positive in 96% (42/44) of FLs and 91% (38/42) of DLBCLs, representing a gain in one case, loss in four cases, and no change in 37 cases through transformation. Bcl-6 was positive in 84% (26/31) of FLs and 88% (28/32) of DLBCLs, representing a gain in four cases, loss in two cases, and no change in 20 cases through transformation. Among 32 DLBCL cases for which both Bcl-2 and Bcl-6 immunohistochemistry could be performed, 25 were Bcl-2+/Bcl-6+, four were Bcl-2+/Bcl-6–, 3 were Bcl-2–/Bcl-6+, and no case was Bcl-2–/Bcl-6–.

The postgerminal center B-cell and plasma cell marker MUM 1 was positive in 16% (5/31) of FLs and in 34% (12/35) of DLBCLs, representing a gain in seven cases, loss in one case, and no change in 20 cases (including four positive cases and 16 negative cases). CD30 was negative in all FLs and positive in 20% (6/30) of DLBCLs. Two cases of DLBCL with anaplastic morphology were positive for CD30. CD30 showed scattered expression in marginally and sparsely distributed large lymphoid cells of low-grade FL and FL grade 3, but no case showed positivity in over 30% of the cells. CD5 was negative in all FLs and positive in only one case (no. 2) of DLBCL. This positive case was FL grade 2 in an abdominal lymph node with a $CD10^+$/Bcl-2+/Bcl-6–/$CD5^-$/cyclin D1-immunophenotype and IGH/BCL2 fusion by FISH analysis initially, and showed transformation to centroblastic monomorphous DLBCL in the tonsil, revealing a $CD10^-$/Bcl-2+/Bcl-6+/$CD5^+$/cyclin D1-immunophenotype and IGH/BCL2 fusion by FISH analysis. In the one case of classical Hodgkin lymphoma after transformation from FL via DLBCL (no. 38), FL in the stomach and esophagus and DLBCL in a cervical lymph node had a $CD20^+$/$CD30^-$/$CD10^+$ phenotype and IGH/BCL2 fusion by FISH analysis, but Hodgkin/Reed-Sternberg cells in an inguinal lymph node had a $CD20^-$/$CD30^+$/$CD15^+$/$CD10^-$ phenotype, and were negative for EBER-1 *in situ* hybridization and positive for IGH/BCL2 fusion by FISH (Fig. 2).

Thirty-one (84%) DLBCLs were classified as GCB, and six (16%) DLBCLs were classified as non-GCB. Two cases of DLBCL (nos. 6 and 7) for which several sequential biopsies were taken were judged from the final biopsy specimen: these were non-GCB in the final DLBCL specimens, but had been GCB in the initial specimens.

FISH analysis. Paraffin-embedded sections were available for 18 FL cases and 34 DLBCL cases. IGH/BCL2 fusion was detected in 89% (16/18) of FL cases and in 82% (28/34) of DLBCL cases. In all six DLBCL cases without IGH/BCL2 fusion, BCL6 translocation was detected in one case (17%). Two FL cases without IGH/BCL2 fusion were not available paraffin-embedded sections.

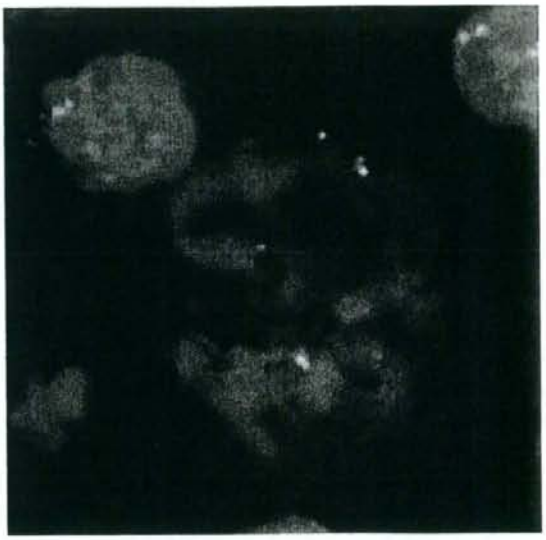

Fig. 2. The result of fluorescence *in situ* hybridization of classical Hodgkin lymphoma transformed from follicular lymphoma (FL). IGH and BCL2 fusion pattern with the LSI IGH Spectrum Green/LSI BCL2 Spectrum Orange Dual Fusion Translocation Probe (Vysis, Downers Grove, IL, USA). Two fusion IGH/BCL2 signals are present.

Statistical analysis. Only the initial treatment regimen was a significant prognostic factor: patients who received CHOP or R-CHOP showed a better outcome than patients who received other treatments ($P < 0.001$). No other significant prognostic factors were detected, including GCB *versus* non-GCB. However, patients with DLBCL showing CD30-positivity (six cases) did not die as a result of disease progression.

Discussion

As transformation of FL to DLBCL is currently the focus of widespread clinical and pathological interests, we studied the

doi: 10.1111/j.1349-7006.2008.00873.x

heterogeneity of the DLBCL component using morphological, immunohistochemical, and FISH analyses.

FL transformed most commonly to the DLBCL centroblastic subtype,[4] but occasionally to the DLBCL anaplastic subtype with CD30 expression.[5] We confirmed that most of the DLBCLs were of the centroblastic subtype, with two exceptional cases of the anaplastic subtype.

CD10 shows restricted expression in germinal center B-cells of reactive lymphoid tissue. Although the reported frequency of CD10 expression in FL varies, about 60% of FLs express CD10.[4] However, no previous report has documented changes in CD10 expression through transformation from low-grade FL to DLBCL. In this study, 14 DLBCLs were negative for CD10, and among them, six showed loss of CD10 expression through transformation. Previous reports have indicated that CD10 expression is often stronger in follicles than in interfollicular neoplastic cells, and that the frequency of CD10 expression is lower in FL grade 3 than in low-grade FL.[24] It is suggested that loss of CD10 expression through FL transformation is possible in the process of escape from the follicular dendritic cell meshwork and diffusion, and tumor cell enlargement.

Bcl-2 is expressed on resting and B and T cells, but not on normal germinal center cells. Bcl-2 protein has an antiapoptotic function,[25] and is expressed in the majority of FLs ranging from nearly 100% in grade 1–75% in grade 3,[26] and in about 30–50% of de novo DLBCLs.[23] Bcl-6 is expressed in germinal center B-cells and a subset of $CD4^+$ T cells.[27] Bcl-6 is expressed in 88% of FLs,[28] and 55–97% of de novo DLBCLs.[29] Most of the DLBCLs that had transformed from FL retained a high frequency of Bcl-2 and Bcl-6 expression, which tended to be higher than that in de novo DLBCL. Because Bcl-2 and Bcl-6 expression was retained during transformation in most cases, Bcl-2 and Bcl-6 positivity might be a precondition for transformation of DLBCL from FL.

MUM1 is a lymphoid-specific member of the interferon regulatory factor family of transcription factors.[30] MUM1 is normally expressed in plasma cells and a minor subset of germinal center B cells, and has been reported to be expressed in 50–77% of DLBCLs.[31–33] In this study, MUM1 was positive in 16% of low-grade FLs and 34% of DLBCLs. This rate was lower than that in de novo DLBCL, but it was surprising that 34% of transformed FLs expressed MUM1. Twenty cases that were MUM1-positive in both the FL and DLBCL components were suggested to be derived from germinal center MUM1-positive B cells, and seven cases showing MUM1-gain indicated that this event was not infrequent during FL transformation.

CD30 was positive in Hodgkin and Reed-Sternberg cells of classical Hodgkin lymphoma, anaplastic large cell lymphoma, anaplastic variant of DLBCL, and a subset of non-neoplastic activated B and T cells.[1,5] Most FLs contain a small number of CD30-positive cells, located mainly at the edge of the neoplastic follicles,[34] and we confirmed this feature. Transformation of FL into CD30-positive large B-cell lymphoma with anaplastic features has been reported.[5] In this study, 20% of the cases gained CD30 expression in DLBCL, which included two cases of the DLBCL anaplastic variant, indicating that CD30-positive large lymphoid cells tended to increase gradually during transformation.

CD5 is reported to be an unfavorable prognostic marker in de novo DLBCL.[35] Richiter's syndrome, a transformant of chronic lymphocytic leukemia/small lymphocytic lymphoma, is a well-known secondary $CD5^+$ DLBCL. Manazza *et al.* reported that CD5 and CD10-double-positive FL transformed to $CD5^+$ DLBCL.[36] Our present study is the first to indicate that $CD5^-$/$CD10^+$ FL with IGH/BCL2 fusion can transform to secondary $CD5^+$/$CD10^-$ DLBCL with IGH/BCL2 fusion.

Notably, our series included one case of classical Hodgkin lymphoma that had transformed from FL via DLBCL. Previous reports have suggested that composite follicular lymphoma and Hodgkin lymphoma represent two morphologic manifestations of the same tumor clones.[8,9] In the present case, IGH/BCL2 fusion was detected in both the FL and the Hodgkin/Reed-Sternberg cells by FISH analysis, strongly suggesting transformation from FL.

Although transformed FL is generally considered to have a GCB phenotype, we demonstrated that a proportion of FLs can show a dramatic change in immunophenotype through transformation. Davies *et al.*[18] examined 35 cases of transformed FL, and found that 89% of them had a GCB phenotype and 9% had a non-GCB phenotype. In our study, six (16%) of the DLBCLs had a non-GCB phenotype. Some previous studies examining the difference in prognosis between patients with a GCB phenotype *versus* those with non-GCB-phenotype DLBCL revealed that the former group had a more favorable prognosis.[15,16] However, Colomo *et al.* found no prognostic difference between them,[37] and recently therefore this issue has been controversial. In the present study, GCB *versus* non-GCB was not a significant prognostic factor. However, as the number of cases was small, further studies are necessary to clarify the prognostic difference between GCB and non-GCB in transformed FL.

We detected a high relative frequency (82%) of IGH/BCL2 fusion in transformed FL. Although the rate is higher than that in Japanese FL, it is almost equal to that in FL grade 1 (10/12, 83%).[21] Because the present cases of DLBCL had transformed from low-grade FL, we were unable to conclude whether cases showing IGH/BCL2 fusion transformed more frequently than cases without it.

In conclusion, our study has clearly demonstrated heterogeneity of the immunophenotype in DLBCL transformed from low-grade FL, suggesting that various mechanisms may affect FL transformation. As many genetic changes including c-MYC amplification and p53 mutation have been detected in transformed FL, it will be necessary to analyze the relationship between these genetic abnormalities and morphological, immunohistochemical, and IGH/BCL2 fusion status in transformed FL.

Acknowledgments

The authors would like to thank C. Kina and S. Miura for technical assistance with immunohistochemistry. This work was supported in part by a Grant-in-Aid for Cancer Research from the Ministry of Health, Labor, and Welfare of Japan.

References

1 A clinical evaluation of the International Lymphoma Study Group Classification of Non-Hodgkin's Lymphoma. The non-Hodgkin's Lymphoma Classification Project. *Blood* 1997; **89**: 3909–18.
2 Horning SJ, Rosenberg SA. The natural history of initially untreated low-grade non-Hodgkin's lymphoma. *N Eng J Med* 1984; **311**: 1471–5.
3 Gallagher CJ, Gregory WM, Jones AE *et al.* Follicular lymphoma: prognostic factors for response and survival. *J Clin Oncol* 1986; **4**: 1470–80.
4 Harris NL, Ferry JA. Follicular lymphoma. In: Knowles DM, ed. *Neoplastic Hematopathology*, 2nd edn. Philadelphia, PA: Lippincott Williams & Wilkins, 2001; 823–53.
5 Alsabeh R, Medeiros LJ, Glackin C *et al.* Transformation of follicular lymphoma into CD30-large cell lymphoma with anaplastic cytologic features. *Am J Surg Pathol* 1997; **21**: 528–36.
6 Yano T, Jaffe ES, Longo DJ *et al.* MYC rearrangements in histologically progressed follicular lymphomas. *Blood* 1992; **80**: 758–67.
7 de Jong D, Voetdujk B, Bavestock G *et al.* Activation of the c-myc oncogene in a precursor B-cell blast crisis of follicular lymphoma, presenting as composite lymphoma. *N Eng J Med* 1998; **318**: 1373.
8 Brauninger A, Hansmann ML, Strickler JG *et al.* Identification of common germinal-center B-cell precursors in two patients with both Hodgkin's disease and non-Hodgkin's lymphoma. *N Eng J Med* 1999; **340**: 1239–47.
9 Marafioti T, Hummel M, Anagnostopoulos I *et al.* Classical Hodgkin's disease and follicular lymphoma originating from the same germinal center B cell. *J Clin Oncol* 1999; **17**: 3804–9.

10 Sander CA, Yano T, Clark HM *et al.* p53 mutation is associated with progression in follicular lymphomas. *Blood* 1993; **82**: 1994–2004.
11 Lo Coco F, Gaidano G, Louie DC *et al.* p53 mutations are associated with histologic transformation of follicular lymphoma. *Blood* 1993; **82**: 2289–95.
12 Pinyol M, Cobo F, Bea S *et al.* p16 (INF4a) gene inactivation by deletions, mutations, and hypermethylation is associated with transformed and aggressive variants of non-Hodgkin's lymphomas. *Blood* 1998; **91**: 2977–84.
13 Elenitoba-Johnson KS, Gascoyne RD, Lim MS *et al.* Homozygous deletions at chromosome 9p21 involving p16 and p15 are associated with histologic progression in follicle center lymphoma. *Blood* 1998; **91**: 4677–85.
14 Tilly H, Rossi A, Stamatoullas A *et al.* Prognostic value of chromosomal abnormalities in follicular lymphoma. *Blood* 1994; **84**: 1043–9.
15 Alizadeh AA, Eisen MB, Davis RE *et al.* Distinct types of diffuse large B-cell lymphoma identified by gene expression profiling. *Nature* 2000; **403**: 503–11.
16 Rosenwald A, Wright G, Chan WC *et al.* The use of molecular profiling to predict survival after chemotherapy for diffuse large B-cell lymphoma. *N Eng J Med* 2002; **346**: 1937–47.
17 Hans SP, Weisenburger DD, Greiner TC *et al.* Conformation of molecular classification of diffuse large B-cell lymphoma by immunohistochemistry using a tissue microarray. *Blood* 2004; **103**: 275–82.
18 Davies AJ, Rosenwald A, Wright G *et al.* Transformation of follicular lymphoma to diffuse large B-cell lymphoma proceeds by distinct oncogenic mechanisms. *Br J Haematol* 2007; **136**: 286–93.
19 Godon A, Moreau A, Talmant P *et al.* Is t(14;18) (q32;q21) a constant finding in follicular lymphoma? An interphase FISH study on 63 patients. *Leukemia* 2003; **17**: 255–9.
20 Biagi JJ, Suymour JF. Insights into the molecular pathogenesis of follicular lymphoma arising from analysis of geographic variation. *Blood* 2002; **99**: 4265–75.
21 Sekiguchi N, Kobayashi Y, Yokota Y *et al.* Follicular lymphoma subgrouping by fluorescence in situ hybridization analysis. *Cancer Sci* 2005; **96**: 77–82.
22 Leoncini L, Delsol G, Gascoyne RD *et al.* Aggressive B-cell lymphomas: a review based on the workshop of the XI meeting of the European association for haematopathology. *Histopathology* 2005; **46**: 241–55.
23 Jaffe ES, Harris NL, Stein H *et al. World Health Organization Classification of Tumors, Pathology and Genetics, Tumours of Haematopoietic and Lymphoid Tissues*. Lyon: IARC Press, 2001; **162–167**: 171–4.
24 Dogan AMQ, Aiello A *et al.* Follicular lymphomas contain a clonally linked but phenotypically distinct neoplastic B-cell population in the interfollicular zone. *Blood* 1998; **91**: 4708–14.
25 Nunez G, London L, Hockenbery D *et al.* Deregulated Bcl-2 gene expression selectively prolongs survival of growth factor-deprived hemoopietic cell lines. *J Immunol* 1990; **144**: 3602–10.
26 Lai R, Arber DA, Chang KL *et al.* Frequency of bcl-2 expression in non-Hodtkin lymphoma: a study of 778 cases with comparison of marginal zone lymphoma and monocytoid B-cell hyperplasia. *Mod Pathol* 1998; **11**: 864–9.
27 Falini B, Fizzotti M, Pileri S *et al.* Bcl-6 protein expression in normal and neoplastic lymphoid tissues. *Ann Oncol* 1997; **8**: 101–4.
28 Peh SC, Shaminie J, Tai YC *et al.* The pattern and frequency of t(14;18) translocation and immunophenotype in Asian follicular lymphoma. *Histopathology* 2004; **45**: 501–10.
29 Anagnostopoulos I, Dallenbach F, Stein H. Diffuse large cell lymphomas. In: Knowles DM, ed. *Neoplastic Hematopathology*, 2nd edn. Philadelphia, PA: Lippincott Williams & Wilkins, 2001; 860.
30 Mamane Y, Heylbroeck C, Genin P *et al.* Interferon regulatory factors: the next generation. *Gene* 1999; **237**: 1–14.
31 Natkunam Y, Warnke RA, Montgomery K *et al.* Analysis of MUM1/IRF4 protein expression using tissue microarrays and immunohistochemistry. *Mod Pathol* 2001; **14**: 686–94.
32 Falini B, Fizzotti M, Pucciarini A *et al.* A monoclonal antibody (MUM1p) detects expression of the MUM1/IRF4 protein in a subset of germinal center B cells, plasma cells, and activated T cells. *Blood* 2000; **95**: 2084–92.
33 Tsuboi K, Iida S, Inagaki H *et al.* MUM1/IRF4 expression as a frequent event in mature lymphoid malignancies. *Leukemia* 2000; **14**: 449–56.
34 Piris M, Gatter KC, Mason DY. CD30 expression in follicular lymphoma. *Histopathology* 1991; **18**: 25–9.
35 Yamaguchi M, Seto M, Okamoto M *et al.* De novo CD5$^+$ diffuse large B-cell lymphoma: a clinicopathologic study of 109 patients. *Blood* 2002; **99**: 815–21.
36 Manazza AD, Bonello L, Pagano M *et al.* Follicular origin of a subset of CD5$^+$ diffuse large B-cell lymphomas. *Am J Clin Pathol* 2005; **124**: 182–90.
37 Colomo L, Lopez-Guillermo A, Perales M *et al.* Clinical impact of the differentiation profile assessed by immunophenotyping in patients with diffuse large B-cell lymphoma. *Blood* 2003; **101**: 78–84.

doi: 10.1111/j.1349-7006.2008.00873.x

Histological and immunophenotypic changes in 59 cases of B-cell non-Hodgkin's lymphoma after rituximab therapy

Akiko Miyagi Maeshima,[1,4] Hirokazu Taniguchi,[1] Junko Nomoto,[2] Dai Maruyama,[2] Sung-Won Kim,[2] Takashi Watanabe,[2] Yukio Kobayashi,[2] Kensei Tobinai[2] and Yoshihiro Matsuno[3]

[1]Clinical Laboratory; [2]Hematology and Stem Cell Transplantation Divisions, National Cancer Center Hospital, Tokyo; [3]Department of Surgical Pathology, Hokkaido University Hospital, Sapporo, Japan

(Received June 30, 2008/Revised September 4, 2008/Accepted September 12, 2008/Online publication November 25, 2008)

Rituximab is a chimeric monoclonal antibody that recognizes the CD20 antigen. It has been used to treat B-cell non-Hodgkin lymphoma (B-NHL), but recently rituximab resistance has been a cause for concern. We examined histological and immunohistochemical changes in 59 patients with B-NHL after rituximab therapy. The patients comprised 32 men and 27 women with a median age of 59 years. Pre-rituximab specimens comprised 34 follicular lymphomas (FL), 11 diffuse large B-cell lymphomas (DLBCL), 10 mantle cell lymphomas, two marginal zone B-cell lymphomas (MZBCL), and two chronic lymphocytic leukemias (CLL). CD20 expression in lymphoma cells was evaluated by immunohistochemistry or flow cytometry. Post-rituximab materials were taken a median of 6 months (4 days to 59 months) after rituximab therapy. Sixteen cases (27%) showed loss of CD20 expression with four histological patterns: pattern 1, no remarkable histological change (FL, 5; DLBCL, 3; and CLL, 2); pattern 2, proliferation of plasmacytoid cells (FL, 2; DLBCL, 1; and MZBCL, 1); pattern 3, transformation to classical Hodgkin's lymphoma (FL, 1); and pattern 4, transformation to anaplastic large cell lymphoma-like undifferentiated lymphoma (FL, 1). Loss of CD20 was unrelated to the interval of biopsies, treatment regimen, clinical response, and frequency of rituximab administration. Loss of CD20 within 1 month of rituximab therapy (3/14, 21%) and regain of CD20 (2/7, 29%) were not frequent. CD20-positive relapse with transformation occurred most frequently in cases of early relapse. In conclusion, B-NHL showed various histological and immunophenotypic changes after rituximab therapy, including not only CD20 loss but also proliferation of plasmacytoid cells or transformation to special subtypes of lymphoma. (*Cancer Sci* 2009; 100: 54–61)

Rituximab is a chimeric monoclonal antibody that has recently been incorporated into the treatment of B-cell non-Hodgkin lymphoma (B-NHL). It recognizes the CD20 antigen, a pan-B-cell marker, binds to it, and induces apoptosis of CD20-positive cells.[1–4] Rituximab can be used as a monotherapy or in combination with conventional chemotherapy for treatment of low- and high-grade, untreated, relapsed, or refractory CD20-positive B-NHL, achieving a high response rate with a low toxicity.

Recent studies have reported that B-NHL show CD20-negative relapse after rituximab therapy.[5–17] Transformation of follicular lymphoma (FL) to CD20-negative diffuse large B-cell lymphoma (DLBCL),[13] proliferation of CD20-negative plasmacytoid tumor cells of marginal zone B-cell lymphoma (MZBCL)[16] or lymphoplasmacytic lymphoma,[13] transformation of FL to classical Hodgkin's lymphoma,[17] and progression of nodular lymphocyte-predominant Hodgkin lymphoma to CD20-negative T-cell-rich B-cell lymphoma have also been reported.[18]

Several mechanisms of resistance to rituximab have been suggested, including selection of a CD20-negative clone as a consequence of rituximab exposure, masking of CD20 epitopes by rituximab itself, or true loss of CD20 antigen by genetic and epigenetic changes.[12,13,15,19–24]

In the present study we carried out retrospective analyses of histological and immunophenotypic changes and outcome in 59 patients with B-NHL after rituximab-containing therapy, to explore the effect of rituximab on CD20 expression and morphology in B-NHL.

Materials and Methods

Patient selection. We reviewed the pathology archives of the National Cancer Center Hospital, Tokyo, Japan, for the period 2002 to 2007. Fifty-nine consecutive cases of CD20-positive B-NHL treated with rituximab, with or without chemotherapy, for which pre- and post-rituximab specimens were available, were included in our study. Rituximab (Zenyaku Kogyo, Tokyo, Japan) was used at a standard dose of 375 mg/m^2 once a week for rituximab monotherapy and once every 3 weeks for the rituximab-cyclophosphamide, doxorubicin, vincristine and prednisone (CHOP) regimen. Clinical information was extracted from the medical records, and the Ann Arbor system was used for staging.

Histological review. Biopsy or surgical specimens were fixed in 10% neutral-buffered formalin overnight, embedded in paraffin, cut into sections 4 μm thick, and stained with hematoxylin–eosin for histological evaluation. All of the pre-rituximab specimens were CD20-positive B-NHL by definition, and post-rituximab specimens included any lymphomas. All of the specimens were reviewed by three pathologists (A.M.M., H.T., and Y.M.) to confirm that the morphological characteristics fulfilled the criteria of the World Health Organization classification of lymphoid neoplasms, 2001.[25] Histological subtype, loss of CD20 expression by immunohistochemistry or flow cytometry, presence or absence of plasmacytoid differentiation, and the relationship between histological transformation and CD20 loss were examined.

Immunohistochemistry, flow cytometry, *in situ* hybridization, and interphase fluorescence *in situ* hybridization analyses. We carried out immunohistochemical staining on formalin-fixed paraffin-embedded pre- and post-rituximab specimens using a panel of monoclonal and polyclonal antibodies. Sections 4 μm thick were cut from each paraffin block, deparaffinized, and incubated

*To whom correspondence should be addressed. E-mail: akmaeshi@ncc.go.jp

doi: 10.1111/j.1349-7006.2008.01005.x

at 121°C in pH 6.0 citrate buffer for 10 min for antigen retrieval. Antibodies included those against the following antigens: CD3 (clone PS1, ×25; Novocastra, Newcastle, UK; polymer method), CD20 (L26, ×100; Dako, Glostrup, Denmark; labeled streptavidin–biotin method [LSAB]), and CD79a (JCB117, ×100; Dako; LSAB) routinely; and CD5 (4C7, ×50, Novocastra; polymer), CD7 (CD7-272, ×100; Novocastra; avidin–biotin complex method [ABC]), CD10 (56C6, ×50; Novocastra; polymer), CD15 (MMA, ×100; Becton Dickinson, Franklin Lakes, NJ, USA; polymer), CD30 (Ber-H2, ×100; Dako; polymer), CD45 (2B11 + PD7/26, ×100; Dako; LSAB), CD45RO (UCHL1, ×50; Dako; LSAB), CD56 (1B6, ×100; Novocastra; LSAB), ALK (ALK1, ×200; Dako; polymer), Bcl-2 (124, ×100; Dako; LSAB), Bcl-6 (poly, ×50; Dako; ABC), cyclin D1 (SP4, ×25; Nichirei, Tokyo, Japan; polymer), TIA-1 (26gA10F5, ×1000; Immunotech, Marseille, France; polymer), granzyme B (GrB-7, ×200; Dako; polymer), MPO (poly, ×1000; Dako; LSAB), MUM1 (MUM1p, ×50; Dako; ABC), PAX5 (24, ×200; Becton Dickinson; ABC), TdT (poly, ×100; Dako; polymer), Igκ (poly, ×20 000; Dako; LSAB), Igλ (poly, ×40 000; Dako; LSAB), IgA (poly, ×100 000; Dako; polymer), IgG (poly, ×20 000; Dako; polymer), and IgM (poly, ×20 000; Dako; polymer) optionally. The percentages of CD20-positive tumor cells were counted semiquantitatively by immunohistochemistry (IHC). Immunoreactivity for CD20 was judged positive (no CD20 loss) if >95% of the tumor cells were stained, partially negative (partial CD20 loss) if 10–95% of the cells were stained, or negative (CD20 loss) if <10% of the cells were stained. When a post-rituximab specimen showed loss of CD20 expression, it was judged as B-cell lineage if there was positivity for CD79a.

Flow cytometry was carried out using an Epics XL-MCL instrument with System II Software (Beckman Coulter). The flow cytometry panel included CD20 (B-Ly1), CD19 (HD37), Igκ (poly), and Igλ (poly) (Dako). Fluorescence *in situ* hybridization (FISH) and *in situ* hybridization (ISH) analyses were optional. Sections 4 μm thick were cut from each paraffin block and used for FISH analysis. Judgment of the fusion gene was carried out as described previously.[26] Dual-color LSI IGH Spectrum Green/LSI BCL2 Spectrum Orange Dual Fusion Translocation Probes (Vysis, Downers Grove, IL, USA) were used to detect t(14;18): IGHBCL2 fusion. ISH with Epstein–Barr-encoded RNA (EBER-1) probes (Dako) was carried out in some cases to detect possible Epstein–Barr virus infection.

Statistical analysis. The relationships between CD20 expression and treatment regimen (rituximab monotherapy vs combination therapy with rituximab and chemotherapy), response (complete response [CR] vs others, or overall response [OR] vs others), frequency of rituximab administration, and interval between the last dose of rituximab and rebiopsy were examined by χ^2-test or Mann-Whitney *U*-test. Differences were considered significant when the *P*-value was less than 0.05.

Results

Patient characteristics. Clinical information for all consecutive 59 patients is summarized in Table 1. The patients comprised 32 men and 27 women, ranging in age from 37 to 80 years with a median age of 59 years. Eight patients had stage I/II disease and 51 patients had stage III/IV disease. All of the patients received rituximab by definition, with or without chemotherapy (CHOP or other types of regimen). The 59 patients received a median of six courses (range 1–17) of rituximab. The median interval between the last dose of rituximab and rebiopsy was 6 months (range 4 days to 59 months). The overall response rate was 79% and the % CR was 46% to rituximab-containing regimens.

Four histological patterns of CD20 loss. The results of histological analysis and immunohistochemical staining for each antibody are summarized in Tables 1–2. The total of 59 pre-rituximab B-NHL specimens included 34 FL with or without a DLBCL component, 11 DLBCL, 10 mantle cell lymphomas (MCL), two MZBCL, and two chronic lymphocytic leukemias (CLL). We considered that the following two factors may have contributed to case selection bias. The first factor is that the date of the approval of rituximab for low-grade B-cell lymphoma preceded that for DLBCL for 2 years in Japan. The second factor is that FL were rebiopsied more frequently than DLBCL because FL relapsed frequently and were followed up for a long time, and checks for transformation to DLBCL were sometimes necessary.

Sixteen cases (27%) showed loss of CD20 expression in post-rituximab specimens by IHC or flow cytometry. The frequencies of CD20 loss in the various histological subtypes were: FL, 26% (9/34); DLBCL, 36% (4/11); MCL, 0% (0/10); MZBCL, 50% (1/2); and CLL, 100% (2/2). Among them, two DLBCL and two FL showed partial loss of CD20 expression. Among the 12 tumors with complete loss of CD20 expression, seven had available flow cytometry data, and all of them showed loss of CD20.

Four patterns of loss of CD20 expression were evident (Table 2): pattern 1, CD20 loss with no remarkable histological change (FL, 5; DLBCL, 3; and CLL, 2) (Fig. 1); pattern 2, proliferation of plasmacytoid cells (FL, 2; DLBCL, 1; and MZBCL, 1) (Fig. 2); pattern 3, transformation to classical Hodgkin lymphoma (FL, 1); and pattern 4, transformation to anaplastic large cell lymphoma (ALCL)-like undifferentiated lymphoma (FL, 1) (Fig. 3). All of the lymphomas after rituximab treatment with pattern 1 or 2 histology were positive for CD79a. Two FL with pattern 2 showed proliferation of plasmacytoid cells, not in the marginal zone but in follicles, as with FL with plasma cells,[27,28] and the plasmacytoid tumor cells were positive for IgM and Igκ by IHC. One DLBCL with pattern 2 was negative for IgM and Igλ by IHC in the pre-rituximab specimen, but positive for them in the post-rituximab specimen. Hodgkin lymphoma with pattern 3, which was previously reported to be a form of transformed FL,[29] was positive for CD30, CD15, and the IGH–BCL2 fusion by FISH, and negative for CD10, CD20, and EBER-1 by ISH. Although we could not determine the lineage of ALCL-like undifferentiated lymphoma with pattern 4, because it was positive for only CD45 and CD45RO and negative for CD3, CD5, CD7, CD10, CD15, CD20, CD30, CD56, CD79a, ALK, bcl-2, bcl-6, granzyme B, MPO, MUM1, PAX5, TdT, TIA-1, and EBER-1 by ISH, it was considered to be transformed FL because of the presence of the IGHBCL2 fusion revealed by FISH in both the pre- and post-rituximab specimens (Fig. 3).

Relationship between rituximab therapy and CD20 expression, and histological changes. The relationships between CD20 expression and interval after the last dose of rituximab, treatment regimens, clinical response, and frequency of rituximab administration were not detected. Among 16 cases showing loss of CD20, the clinical response to treatment was no change (NC) in three cases, and CR or partial response (PR) in the others.

Fourteen patients underwent rebiopsy within 1 month of the last dose of rituximab. Among them, only three cases (21%) were negative for CD20. Seven cases showing loss of CD20 expression after rituximab therapy were subsequently observed and rebiopsied and, among them, two cases (cases FL4-2 and FL8) regained CD20 expression at 7 and 15 months after the last dose of rituximab. The other five cases were found not to have regained CD20 expression at 2, 7, 12, 28, and 44 months after the last dose of rituximab.

Nine patients with FL achieved CR or PR after treatment with a rituximab-containing regimen, but their lymphomas showed early relapse (within 3 months to 1 year later). Among them, five cases (cases FL12, FL18, FL25, FL33, and FL34) relapsed as CD20-positive DLBCL, two (cases FL16 and FL21) as CD20-positive low-grade FL, one (case FL3-2) as CD20-negative FL grade 2, and one (case FL8) as transformation to Hodgkin's lymphoma.

Table 1. Patient characteristics

Case	Age (years)/sex	Stage	Pre-rituximab diagnosis (sample)	Therapy and response between biopsy and operation	Post-rituximab diagnosis (sample)	Post-rituximab interval (months)†	CD20 expression (%)	Histology by immunohistochemistry	Pattern
FL1	55/M	4	FL, gr.2 (LN)	Rx4, NC	FL, gr.1 (BM)	3	0	NHC	1
FL2	52/M	4	FL, gr.2 (LN)	C-MOPPx8, PR, Rx4, NC	FL, gr.1 (BM)	22	0	NHC	1
FL3-1	52/M	3	FL, gr.1 (LN)	R-CHOPx6, CR	FL, gr.2 (BM)	33	100	NHC	
FL3-2				Rx8+C-MOPPx5, CR, relapse, R-ICEx2, PR	FL, gr.2 (LN)	6	0	NHC	1
FL4-1	42/F	4	FL, gr.1 (LN)	Rx8+C-MOPPx16, NC	FL, gr.1 (BM)	23	100	NHC	
FL4-2				Rx8, NC	FL, gr.1 (BM)	5 days	0	NHC	1
FL5	59/M	4	FL, gr.2 (LN)	Rx4, NC, C-MOPPx13, PD, R-C-MOPPx8, CR	FL, gr.2 (BM)	21	–‡	NHC	1
FL6	40/M	4	FL, gr.1 (LN)	R-CHOPx6, CR	FL, gr.2 (LN)	12	90	Partially plasmacytoid cells (IgM+/Igκ+/CD138–)	2
FL7	49/F	4	FL, gr.1 (duodeunum)	R-CHOPx6, CR	FL, gr.1 (LN)	17	90	Partially plasmacytoid cells (IgM+/Igκ+/CD138–)	2
FL8	61/F	4	DLBCL+FL, gr.3a (LN)	Rx4+CHOPx8, CR	HL, MC (LN)	11	0	Transformation to HL	3
FL9	68/M	4	FL, gr.2 (LN)	R-C-MOPPx6, R-C-MOPPx8, relapse, fludarabine + Rx3	ALCL-like (liver)	18 days	0	Transformation to ALCL-like	4
L10	76/F	4	FL, gr.2 (LN)	Rx8, NC	FL, gr.2 (BM)	6	100	NHC	
FL11	54/F	4	FL, gr.2 (LN)	R-CHOPx6, CR	FL, gr.1 (BM)	15 days	100	NHC	
FL12	40/F	4	FL, gr.1 (LN)	CHOPx6, CR, relapse, C-MOPPx4, NC, Rx4, CR	DLBCL (colon)	4	100	Transformation to DLBCL	
FL13	44/M	4	FL, gr.2 (LN)	R-CHOPx6, PR, C-MOPPx6 radiation, PR	DLBCL+FL, gr.1 (BM)	59	100	Transformation to DLBCL	
FL14	47/M	4	FL, gr.2 (LN)	COPPx6, NC, Rx4, PD	FL, gr.1 (BM)	1	100	NHC	
FL15	43/M	4	FL, gr.1 (LN)	Rx4+C-MOPPx2, CR, zevalin, CR	FL, gr.1 (orbit)	26	100	NHC	
FL16	61/F	4	FL, gr.1 (BM), DLBCL (skin)	R-CHOPx8, CR	FL, gr.2 (LN)	9	100	NHC	
FL17	48/F	4	FL, gr.2 (LN)	Rx4+CHOPx6, PR	FL, gr.1 (BM)	23	100	NHC	
FL18	60/F	3	FL, gr.2 (LN)	Rx4, CR	DLBCL (tonsil)	4	100	Transformation to DLBCL	
FL19	54/F	4	FL, gr.1 (BM, stomach)	R-CHOPx6, PR	FL, gr.1 (BM)	37	100	NHC	
FL20	54/F	4	FL, gr.1 (LN)	Rx4, PR, CHOPx8, PR	FL, gr.2 (cecum)	36	100	NHC	
FL21	61/F	4	FL, gr.2 (LN)	R-CHOPx8, PR	FL, gr.1 (BM)	5	100	NHC	
FL22	66/F	3	FL, gr.2 (LN)	R-CHOPx8, PR	FL, gr.2 (skin)	26	100	NHC	
FL23	53/F	4	FL, gr.2 (ileum, colon)	R-CHOPx8, NC	FL, gr.1 (duodenum)	10	100	NHC	
FL24	51/F	4	FL, gr.2 (duodenum)	Rx1 (within R-CHOP)	FL, gr.1 (duodenum)	4 day	100	NHC	
FL25	55/M	3	DLBCL+FL, gr.3b (LN)	R-CHOPx8, CR	DLBCL (LN)	3	100	NHC	
FL26	37/M	4	FL, gr.2 (LN)	Rx2 (within R-CHOP)	FL, gr.2 (duodenum)	8 days	100	NHC	
FL27	62/M	4	FL, gr.1 (ileum)	Rx3 (within R-CHOP)	FL, gr.1 (duodenum)	8 days	100	NHC	
FL28	57/F	4	FL, gr.3a (LN)	Rx4, NC	DLBCL (LN)	3	100	Transformation to DLBCL	
FL29	51/M	3	DLBCL+FL, gr.3b (LN)	R-CHOPx6+Rx8, CR	DLBCL (LN)	21 days	100	NHC	
FL30	60/M	1	FL, gr.1 (duodenum)	Rx8, CR	FL, gr.1 (duodenum)	4 days	100	NHC	
FL31	63/M	1	FL, gr.1 (duodenum)	Rx8, PR	FL, gr.1 (duodenum)	1	100	NHC	
FL32	75/F	4	FL, gr.1 (BM)	Rx3	FL, gr.1 (BM)	4 days	100	NHC	
FL33	77/M	4	DLBCL+FL, gr.3a (pharynx)	R-CHOPx8, CR	DLBCL (LN)	8	100	NHC	

doi: 10.1111/j.1349-7006.2008.01005.x

Table 1. Continued

Case	Age (years)/sex	Stage	Pre-rituximab diagnosis (sample)	Therapy and response between biopsy and operation	Post-rituximab diagnosis (sample)	Post-rituximab interval (months)†	CD20 expression (%)	Histology by immunohistochemistry	Pattern
FL34	65/M	3	FL, gr.3a (LN)	Rx8, CR	DLBCL (LN)	5	100	Transformation to DLBCL	
DLBCL1-1	47/M	2	DLBCL (right testis)	R-CHOPx8, CR	DLBCL (left testis)	2	100	NHC	
DLBCL1-2				R-IVACx3, CR, BMT, CR	DLBCL (BM)	4	0	NHC	1
DLBCL2	71/M	3	DLBCL (ileum)	R-CHOPx8, CR, Rx1	DLBCL (LN)	10 days	10	NHC	1
DLBCL3	55/M	4	DLBCL (tonsil)	R-CHOPx8, PR	DLBCL (LN)	3	70	NHC	1
DLBCL4	58/F	2	DLBCL (EBER-1+) (stomach)	R-CHOPx8, PR	DLBCL (stomach)	4	0	Plasmacytoid cells (IgM+/Igλ+/CD138–)	2
DLBCL5	80/M	2	DLBCL (LN)	R-CHOPx8, CR	DLBCL (subcutaneous)	6	100	NHC	
DLBCL6	60/F	4	DLBCL (breast)	Chemotherapy, Rx4, CR	DLBCL (breast)	29 days	100	NHC	
DLBCL7	61/F	2	DLBCL (tonsil)	R-EPOCHx4, CR	DLBCL (colon, rectum)	16	100	NHC	
DLBCL8	75/F	4	DLBCL (stomach,duodenum)	R-CHOPx8, CR	DLBCL (stomach, duodenum)	30	100	NHC	
DLBCL9	65/F	3	DLBCL (LN)	Rx8+CHOPx6, PD	DLBCL (LN)	3	100	NHC	
DLBCL10	64/M	2	DLBCL (stomach)	Rx1+CHOPx2 (within R-CHOP)	DLBCL (stomach)	20 days	100	NHC	
DLBCL11	63/M	2	DLBCL (LN)	Rx8+CHOPx5+radiation, CR	DLBCL (LN)	8	100	NHC	
MCL1	72/M	4	MCL (LN)	R-CHOPx4, PR, Rx4, NC, COPx6, PD, R-CNOPx6, PD, cladribine, PD	MCL (stomach)	10 days	100	NHC	
MCL2	76/M	4	MCL (LN)	R-CHOPx8, PR	MCL (BM)	20	100	NHC	
MCL3	68/M	4	MCL (BM)	Rx1+CHOPx6, PR	MCL (BM)	1	100	NHC	
MCL4	66/M	4	MCL (colon)	R-CHOPx8, CR	MCL (stomach)	30	100	NHC	
MCL5	55/M	4	MCL (tonsil)	Rx4, PR	MCL (tongue)	28	100	NHC	
MCL6	59/F	4	MCL (stomach)	Rx4, PR, C-MOPPx8+ radiation+COP, PD	MCL (bone)	21	100	NHC	
MCL7-1	63/F	4	MCL (LN)	Rx4+C-MOPPx8, CR	MCL (stomach, duodenum)	17	100	NHC	
MCL7-2				Rx4, PR	MCL (stomach)	1	100	NHC	
MCL8	54/F	4	MCL (ileum)	Rx8+CHOPx6, CR	MCL (small intestine)	3	100	NHC	
MCL9	78/M	4	MCL (stomach)	Rx8, PD	MCL (orbit)	2	100	Change to blastoid variant	
MCL10	70/M	4	MCL (LN)	R-CHOPx8, PR	MCL (stomach)	18	100	NHC	
MZBCL1	68/F	3	MZBCL (LN)	R-ICEx1, CR	MZBCL (tonsil)	15	0	Plasmacytoid cells	2
MZBCL2	55/M	4	MZBCL (BM)	R-CHOPx6, PR	MZBCL (BM)	4	100	NHC	
CLL1	54/M	4	CLL (BM)	Rx2+C-MOPPx6, PR	CLL (LN)	12 days	0	NHC	1
CLL2	52/F	4	CLL (BM)	CHOPx8, COPx10, R-CEPPx7, R-ESHAPx2, CHASEx2, R-ESHAP+PBSCT, Rx5, PR	CLL (BM)	11	0	NHC	1

†From last dose of rituximab; ‡by flow cytometry. ALCL, anaplastic large cell lymphoma; BM, bone marrow; BMT, bone marrow transplantation; CEPP, cyclophosphamide, etoposide, procarbazine, and prednisolone; CHASE, cyclophosphamide, cytosine arabinoside, etoposide, and dexamethasone; CHOP, cyclophosphamide, doxorubicin, vincristine, and prednisone; CLL, chronic lymphocytic leukemia; C-MOPP, cyclophosphamide, vincristine, prednisone, and procarbazine; CR, complete response; diff., differentiation; DLBCL, diffuse large B-cell lymphoma; EPOCH, etoposide, prednisone, vincristine, cyclophosphamide, and doxorubicin; ESHAP, etoposide, methylprednisolone, high-dose cytarabine, and cisplatin; FL, follicular lymphoma; HL, Hodgkin's lymphoma; ICE, ifosfamide, carboplatin, and etoposide; IVAC, ifosfamide, vincristine, and cytarabine; LN, lymph node; MC, mixed cellularity; MCL, mantle cell lymphoma; MZBCL, marginal zone B-cell lymphoma; NC, no change; NHC, no remarkable histological change; PBSCT, peripheral blood stem cell transplantation; PD, progressive disease; PR, partial response; R, rituximab.

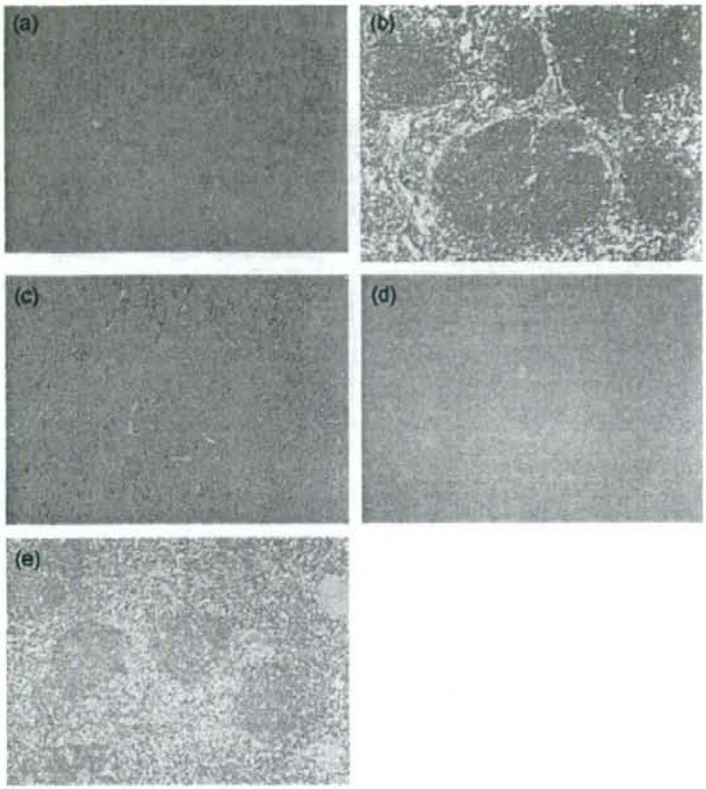

Fig. 1. (a–e) A case of pattern 1 change in CD20-positive follicular lymphoma (FL) to CD20-negative FL. FL, grade 1, (a) in a lymph node (hematoxylin–eosin, ×40) and (b) with CD20-positive phenotype, pre-rituximab (×100). FL, grade 2, (c) in a lymph node (hematoxylin–eosin, ×40) with (d) CD20-negative (×40) and (e) CD79a-positive (×40) phenotypes, post-rituximab.

Table 2. Four histological patterns of loss of CD20 expression after rituximab therapy

Histological pattern	Distribution
Pattern 1: loss of CD20 with no remarkable histological change	FL, 5; DLBCL, 3; CLL, 2
Pattern 2: proliferation of plasmacytoid cells	FL, 2; DLBCL, 1; MZBCL, 1
Pattern 3: transformation to classical Hodgkin lymphoma	FL, 1
Pattern 4: transformation to anaplastic large cell lymphoma-like undifferentiated lymphoma	FL, 1

CLL, chronic lymphocytic leukemia; DLBCL, diffuse large B-cell lymphoma; FL, follicular lymphoma; MZBCL, marginal zone B-cell lymphoma.

Discussion

Recent reports have indicated that the treatment of B-NHL with rituximab may be associated with CD20-negative lymphoma relapse,[5–17] and the frequency of loss of CD20 after rituximab treatment varies widely (24, 56, 60, and 94%).[9,11,13,14] In the present study, 16 of 59 B-NHL (27%) showed loss of CD20 after rituximab-containing therapy using a larger series than in previous reports. Our results also suggested that the frequency of CD20 loss was not largely affected by the period before rebiopsy. Although the site of sampling (bone marrow vs non-bone marrow) might affect the observed degree of CD20 loss,[9] this issue needs to be studied further using a larger number of cases. Tumors with loss of CD20 in the present study included FL, DLBCL, MZBCL, and CLL. Although Goteri *et al.* reported that MCL frequently showed loss of CD20 expression in bone marrow, none of our MCL cases showed CD20 loss.[13] Because a previous report indicated that rituximab + CHOP combination therapy (R-CHOP) had insufficient efficacy for MCL,[30] it was considered that this regimen might not have been sufficiently potent to induce selection of a CD20-negative clone.

Four histological patterns of CD20 loss were evident. The majority were patterns 1 or 2, whereas patterns 3 or 4 were rare. Recently, several reports have described relapse with pattern 1 or 2 histology after rituximab therapy.[13,16] Using flow cytometry, Goteri *et al.* demonstrated that 26 cases of low-grade B-cell lymphoma showed CD20 loss in bone marrow aspirates, including cases with no histological change, and with residual plasmacytoid tumor cells of lymphoplasmacytic lymphoma.[13] It has also been reported that mucosa-associated lymphoid tissue lymphoma changes to a pure plasma-cell neoplasm.[16]

Case FL8, which showed transformation to Hodgkin lymphoma (pattern 3), was one of the transformed FL that we reported previously.[29] As composite Hodgkin lymphoma and FL is reported to be very rare,[31,32] rituximab might have induced transformation to Hodgkin lymphoma. Recently, a case

doi: 10.1111/j.1349-7006.2008.01005.x

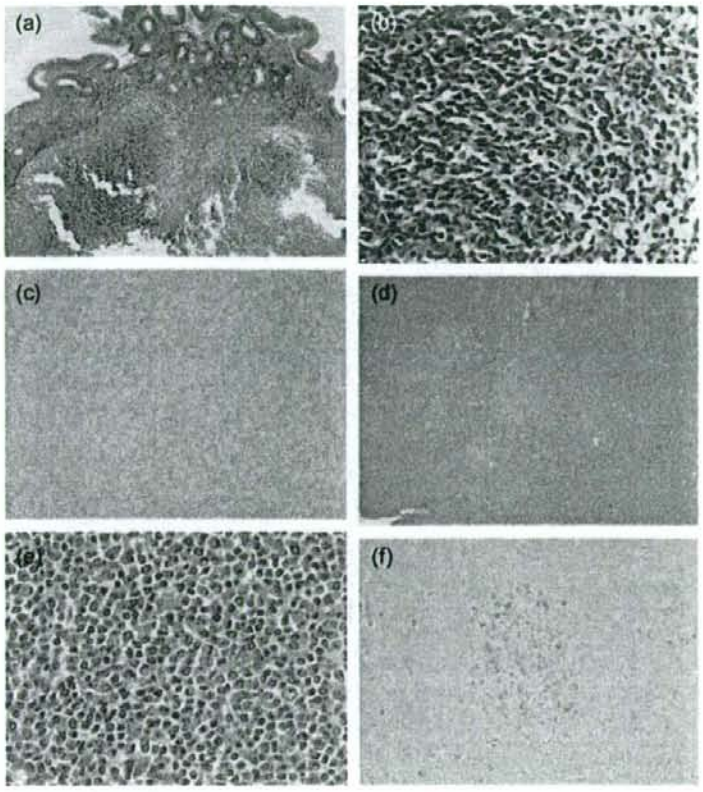

Fig. 2. (a–f) A case of pattern 2 change of follicular lymphoma (FL) to FL with plasma cells. FL, grade 1 in duodenum (hematoxylin–eosin), (a) ×40, (b) ×400, with (c) IgM-negative phenotype (×100), pre-rituximab. FL, grade 1 with plasmacytoid differentiation in lymph node (hematoxylin–eosin), (d) ×40, (e) ×400, with (f) IgM-positive phenotype (×100), post-rituximab.

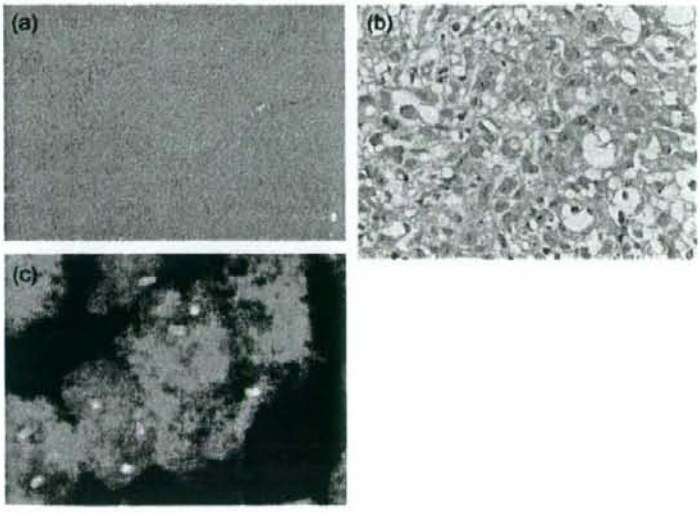

Fig. 3. (a–c) A case of pattern 4 change of follicular lymphoma (FL) to anaplastic large-cell lymphoma (ALCL)-like undifferentiated lymphoma. (a) FL, grade 2 in lymph node, pre-rituximab (hematoxylin–eosin, ×40). (b) ALCL-like undifferentiated lymphoma in liver, post-rituximab (hematoxylin–eosin, ×400). (c) The result of fluorescence *in situ* hybridization of ALCL-like undifferentiated lymphoma. IGH and BCL2 fusion pattern. Two fusion IGHBCL2 signals were present.